

# One Centimetre Receiver Array-prototype observations of the CRATES sources at 30 GHz

M. W. Peel<sup>1</sup>, M. P. Gawroński<sup>2</sup>, R. A. Battye<sup>1</sup>, M. Birkinshaw<sup>3</sup>, I. W. A. Browne<sup>1</sup>, R. J. Davis<sup>1</sup>, R. Feiler<sup>2</sup>, A. J. Kus<sup>2</sup>, K. Lancaster<sup>3</sup>, S. R. Lowe<sup>1</sup>, B. M. Pazderska<sup>2</sup>, E. Pazderski<sup>2</sup>, B. F. Roukema<sup>2</sup> and P. N. Wilkinson<sup>1</sup>

<sup>1</sup> Jodrell Bank Centre for Astrophysics, The University of Manchester, Manchester, M13 9PL

<sup>2</sup> Toruń Centre for Astronomy, Nicolaus Copernicus University, 87-100 Toruń/Piwnice, Poland

<sup>3</sup> University of Bristol, Tyndall Avenue, Bristol, BS8 ITL

Accepted 2010 September 4. Received 2010 September 1; in original form 2010 July 29

## ABSTRACT

Knowledge of the population of radio sources in the range  $\sim 2 - 200$  GHz is important for understanding their effects on measurements of the Cosmic Microwave Background power spectrum. We report measurements of the 30 GHz flux densities of 605 radio sources from the Combined Radio All-sky Targeted Eight-GHz Survey (CRATES), which have been made with the One Centimetre Receiver Array prototype (OCRA-p) on the Toruń 32-m telescope. The flux densities of sources that were also observed by WMAP and previous OCRA surveys are in broad agreement with those reported here, however a number of sources display intrinsic variability. We find a good correlation between the 30 GHz and Fermi gamma-ray flux densities for common sources. We examine the radio spectra of all observed sources and report a number of Gigahertz-peaked and inverted spectrum sources. These measurements will be useful for comparison to those from the Low Frequency Instrument of the *Planck* satellite, which will make some of its most sensitive observations in the region covered here.

**Key words:** Astronomical data bases: miscellaneous – Galaxies: statistics – Galaxies: active – Cosmology: observations

## 1 INTRODUCTION

Emission from blazars dominates the high latitude sky at high radio frequencies and also at gamma-ray frequencies. Blazars are a major foreground contaminant of observations of the Cosmic Microwave Background (CMB), particularly at high multipoles. In order to subtract effects of such objects from CMB observations, it is necessary to know the flux densities of individual bright sources as well as the statistical properties of the overall source population. Knowledge of the brightest individual sources comes directly from the CMB surveys themselves. WMAP has detected sources down to  $\sim 0.5$  Jy at 22–93 GHz (Gold et al. 2010) and the more sensitive Low Frequency Instrument (LFI) in the *Planck* satellite will detect sources with flux densities of a few hundred mJy at 33, 44 and 70 GHz. However, a knowledge of the statistical properties of significantly weaker sources is desirable.

At the present time there are no point source surveys with the appropriate combinations of flux density limit and frequencies to understand the contaminating effect that these sources have on CMB experiments such as *Planck*. Thus at present one must rely on measuring the high fre-

quency properties of sources selected from lower frequency surveys in order to infer the high frequency population statistics. We have a programme aimed at characterising the high frequency radio source population in total intensity (Lowe et al. 2007; Gawroński et al. 2010) and polarisation (Jackson et al. 2010; Battye et al. 2010). The present paper is the latest in this series, being intermediate in flux density between the strong ( $>350$  mJy at 4.85 GHz) Caltech-Jodrell Bank flat-spectrum (CJF) sample (Lowe et al. 2007) and the weaker Very Small Array (VSA) sources (Gawroński et al. 2010).

The Combined Radio All-sky Targeted Eight GHz Survey (CRATES; Healey et al. 2007) is a sample of  $\sim 11\,000$  strong flat spectrum sources with measured flux densities at 8.4 GHz. CRATES is currently the most complete large-area, flat spectrum point source sample at flux densities of hundreds of mJy. It samples a flux density range starting over an order of magnitude lower than the WMAP source sample (Gold et al. 2010). Thus CRATES sources represent excellent targets to follow up at higher frequencies.

The CRATES sample was originally selected to study blazars – radio-loud Active Galactic Nuclei in which the

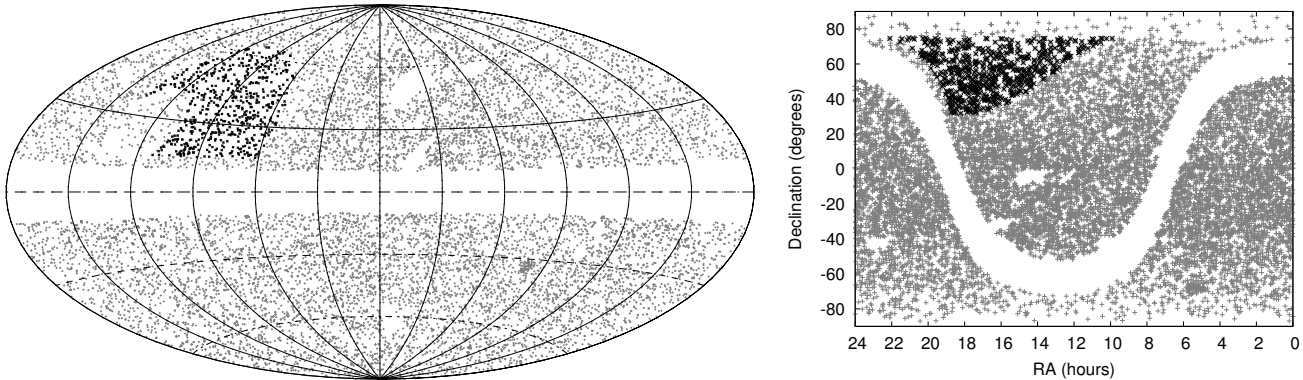


**Figure 1.** The distribution of CRATES sources in Galactic coordinates in Aitoff equal-area projection centred on  $l = 0^\circ$  (left) and in RA and Dec (right). The complete CRATES sample is shown in grey. The sample observed by OCRA is shown in black. The small cluster of sources at low declination is the Large Magellanic Cloud, and the empty areas below Dec  $0^\circ$  are where there are gaps in the 4.8 GHz observation coverage (Healey et al. 2007). The reduced number of sources above  $75^\circ$  is caused by the upper declination limit in the GB6 observations.

relativistic jet axis points close to the observer's line of sight. This angle of observation means that the emission is Doppler boosted such that the received flux densities are dramatically increased compared to what would be observed at larger angles to the jet axis. This beamed non-thermal emission stretches from radio to gamma-ray frequencies. Blazars dominate the high Galactic latitude gamma-ray source counts produced by the Fermi Gamma-ray Space Telescope (Abdo et al. 2010a,b) and many will be detected by Planck, SCUBA2 and Herschel. Thus, in addition to their usefulness for CMB studies, there is the potential to produce well-sampled spectral energy distributions. An important motivation for our work is to contribute to this undertaking with our high radio frequency flux density measurements.

Sources contained in CRATES are those most likely to contaminate *Planck* measurements of the CMB. Observations of these sources at 30 GHz using the OCRA-p receiver on the Toruń 32-m telescope, as described in this paper, could potentially be used to subtract the sources from the 30 GHz Low Frequency Instrument (LFI) maps, and will be useful for cross-comparison with the source lists generated by the *Planck* High Frequency Instrument (HFI). In the northern hemisphere, *Planck* will make its most sensitive observations at the north ecliptic pole, hence this is the best field in which to observe a sub-sample of the CRATES sources.

## 2 SUBSAMPLE SELECTION

The CRATES source sample consists of extragalactic sources ( $|b| > 10^\circ$ ) that have spectral indices between 1.4 and 4.8 GHz of  $\alpha > -0.5$  (where  $S \propto \nu^\alpha$ ), and have 4.8 GHz fluxes greater than 65 mJy. In the northern hemisphere the CRATES sample was selected from the 4.85 GHz GB6 catalogue (Gregory et al. 1996) making use of 1.4 GHz flux densities from the NRAO VLA Sky Survey (NVSS; Condon et al. 1998) to select only the flat spectrum sources, i.e. those with spectral index  $\alpha_{1.4}^{4.8} > -0.5$ . CRATES is essentially a subset of the Cosmic Lens All-Sky Survey (CLASS; Myers et al. 2003; Browne et al. 2003) combined with other surveys from the southern hemisphere. It should also be noted

that at declinations above  $75^\circ$ , where GB6 is incomplete, it may be missing significant numbers of sources; efforts to improve its completeness are ongoing (Healey et al. 2009). The complete sample contains  $\sim 11\,000$  sources.

The subsample observed with OCRA has a series of additional selection criteria. We require that the sources:

- are closer than  $35^\circ$  from the North Ecliptic Pole (located at RA  $18^\text{h}$  Dec  $\sim 66.5^\circ$ );
- are at Dec  $< 75^\circ$  (the GB6 survey limit);
- are no closer than  $15^\circ$  to the Galactic plane ( $|b| > 15^\circ$ );
- have a measured 8.4 GHz flux density.

This selection yields 754 “sources”. However, the CRATES catalog sometimes lists several components belonging to a single source, which would all lie within the 1.2 arcmin OCRA beam. For all CRATES entries with multiple components closer together than 1 arcmin we added their 8.4 GHz flux densities together. Most of the 149 extra components are very close to the main component (63 are within 0.1 arcmin and 120 are within 0.5 arcmin). They are also substantially lower in flux density than the main components (typically a few mJy at 8.4 GHz), and as such merging the multiple components together should negligibly affect the source spectral indices. The position of the brightest component is used as the pointing position for our observations. Our final target-list contains 605 sources.

The RA range of the source sample is  $9^\text{h} 54^\text{m}$  to  $22^\text{h} 6^\text{m}$ ; the declination range is from  $31^\circ 44'$  to  $74^\circ 57'$ . The 605 CRATES sources within this sample are shown in black in Figure 1, with all of the rest of CRATES sources shown in grey.

## 3 OCRA-P OBSERVATIONS

OCRA-p is a two-beam 30 GHz instrument mounted on the 32-m Toruń telescope. It is the first instrument of the OCRA programme (Browne et al. 2000). This two-beam pseudo-correlation receiver is based upon the Planck LFI receiver chain, and is also similar in concept to the WMAP 23 GHz receiver. With an overall system temperature of 40 K, and a bandwidth of 6 GHz, the receiver has a sensitivity of

$6 \text{ mJy s}^{1/2}$ . It has previously been used to observe strong radio sources (Lowe et al. 2007), planetary nebulae (Pazderska et al. 2009), weak radio sources (Gawroński et al. 2010) and clusters of galaxies by the Sunyaev-Zel'dovich Effect (Lancaster et al. 2007, 2010). The OCRA-p data reduction process is described in detail in Gawroński et al. (2010) and Peel (2009).

In order to optimise the observing efficiency an expected flux density of each source at 30 GHz was calculated from an extrapolation from the 4.8 and 8.4 GHz flux densities. Those sources that were predicted to be stronger than 100 mJy were observed using cross-scan measurements, first in elevation then in azimuth, as described in Lowe et al. (2007) and Gawroński et al. (2010). As cross-scan measurements provide simultaneous pointing corrections for the telescope, these are robust flux density measurements. A different strategy is used for sources  $< 100 \text{ mJy}$ , which may be too faint for reliable cross-scan observations in the face of atmospheric fluctuations. For these objects, following a cross-scan pointing observation on a nearby bright and unresolved source closer than  $4^\circ$  to the fainter source, a set of “on-off” measurements are carried out, where the two beams of the instrument are alternately pointed towards the source position, as described in Gawroński et al. (2010). Any source not detected using the cross-scan method was re-observed using on-off measurements. This combination of the two observational techniques provides the most efficient route to flux density measurements with OCRA-p.

As OCRA-p is sensitive to a single linear polarisation, measurements of the flux density of polarised sources will vary depending on the hour angle of the observation. However, as flat spectrum radio sources are only weakly polarised at high frequencies ( $\sim 3$  per cent; see e.g. Jackson et al. 2010) this will not be a significant effect compared to the intrinsic source variability and the measurement uncertainty.

We use the planetary nebula NGC 7027 for primary flux density calibration. This has been measured at 33 GHz by Hafez et al. (2008), who report a flux density of  $5.39 \pm 0.04 \text{ Jy}$  at an epoch of 2003.0 with a secular decrease of  $-0.17 \pm 0.03$  per cent per year. Extrapolating this to 2009.0 yields a flux density of  $5.34 \pm 0.04 \text{ Jy}$ , which can then be scaled to 30 GHz using the quoted spectral index of -0.119 to give  $5.40 \pm 0.04 \text{ Jy}$ . We note that observations of NGC 7027 by Zijlstra et al. (2008) are consistent with Hafez et al. (2008). The absolute calibration used by Hafez et al. (2008) was the 5-year WMAP brightness temperature for Jupiter of  $146.6 \pm 0.8 \text{ K}$  (Hill et al. 2009). We note that there is a debate about the effect of potential timing errors, which could affect the flux density scale at the  $\sim 0.2\%$  level (Roukema 2010, and references therein).

Secondary flux density calibration is carried out using a signal from a noise diode measured after each source observation. We correct for the changes in system gain as a function of elevation using a series of measurements of NGC 7027 at different elevations. We also correct for atmospheric absorption based on measurements of the system temperature at zenith and  $60^\circ$  from the zenith.

Observations commenced in November 2008 and were completed in June 2010. A total of 4,105 separate observations have been made – an average of 6.8 measurements per source, with each source having at least 3 good measurements.

Cross-scan measurements where the amplitudes recorded from the two beams disagree by greater than 20 per cent, or where the widths of the peaks disagree by greater than 40 per cent, are flagged and removed from the analysis. Measurements that are obviously affected by poor weather are manually flagged. We also automatically flag any on-off measurements with an error on the measurement that is both over 7 mJy and greater than 15 per cent of the flux density of the measurement. Additionally, measurements that are clearly erroneously low are manually flagged as these are likely to have been caused by the telescope not being positioned accurately on the source. In total, 1,104 measurements have been flagged; 3001 measurements, or an average of 5 per source, are used in the final analysis.

The reported errors on the OCRA-p flux density measurements were calculated using the weighted standard deviation of the unflagged measurements of each source, where the weights were determined using the uncertainty in the least-squares fits to the cross-scan measurements or the scatter of the 1 second samples within the on-off measurements (see Gawroński et al. 2010; Peel 2009 for more details).

To compensate for the effects of small random pointing errors in the on-off measurements, we have increased the measured flux density for on-off measurements for the CRATES sample by 5 per cent. This is an empirical number determined from a sample of sources where we made measurements using both methods. We also quadratically add 5 per cent of the measured flux density to the measurement error to account for the pointing uncertainty during on-off measurements.

As with the VSA sources (Gawroński et al. 2010), the final error on the flux density for each source is calculated by  $\sigma = \sqrt{\sigma_{\text{meas}}^2 + (0.08S)^2}$  where the 8 per cent of the flux density takes into account the uncertainty due to calibration, atmospheric and gain-elevation corrections and other atmospheric effects (e.g.  $1/f$ -like fluctuations).

## 4 FLUX DENSITIES

The flux densities of the CRATES source subsample as measured with OCRA-p are listed in Table 3. The 1.4, 4.8 and 8.4 GHz flux densities from the CRATES source catalogue are also listed. We have made a machine readable copy of the flux density table, as well as plots of the measurements of each source over time and the aggregated source spectra between 26 MHz and 150 GHz, available online at <http://www.jodrellbank.manchester.ac.uk/research/ocra/crates/>.

From an inspection of NVSS (Condon et al. 1998), FIRST (Becker et al. 1995) and CLASS (Myers et al. 2003; Browne et al. 2003) data it is clear that the majority of the CRATES sources are unresolved. A number do, however, show extension and/or multiple components; these are marked with an “e” in Table 3. Sources where multiple components listed in CRATES have been merged together are denoted “NC” where “N” is the number of components. WMAP sources (Gold et al. 2010) are marked with a “w”, CJF sources (Taylor et al. 1996; Lowe et al. 2007) are marked with a “c” and Fermi point sources (Abdo et al. 2010a) are marked with an “f” (see the next section). Potential Gigahertz Peaked Spectrum (GPS) sources are marked with a “g” (see Section 6). We note that there are two CLASS lens

systems within the sample – J1609+6532 and J1938+6648 (Browne et al. 2003).

There are 42 sources that appear variable within the OCRA measurements; these are marked with a “v” in Table 3. Sources were identified as variable if they are reasonably strong ( $>20$  mJy) and have two measurements which are 25 per cent higher than the mean. Although sources with two measurements that are 25 per cent lower than the mean could also be variable sources, these will be more contaminated by any sources with measurements that suffer from bad telescope pointing (and hence a reduced measured flux density) that have not been flagged. As such, we do not include these in the list of variable sources.

## 5 COMPARISON WITH OTHER MEASUREMENTS

### 5.1 CJF Sources

There are 87 sources in common between the CRATES subsample and the OCRA-p measurements of CJF sources reported in Lowe et al. (2007); the flux densities of these are plotted in Figure 2. There is broad agreement between the two, although there is a large degree of scatter.

Four of the sources have particularly discrepant flux densities (by a factor greater than 2), which can be certainly ascribed to intrinsic variability. J1849+6705 has increased in flux density from  $575 \pm 29$  mJy in Lowe et al. (2007) to  $3675 \pm 301$  mJy. J1852+4855 was  $196 \pm 11$  mJy, and is now  $530 \pm 49$  mJy. J2006+6424 was  $234 \pm 12$  mJy; it is now  $1143 \pm 93$  mJy. Finally, J0954+7435 was  $738 \pm 106$  mJy and has now decreased to  $101 \pm 12$  mJy. This last type of source behaviour could present significant problems for non-contemporaneous measurements of point sources for subtraction from CMB maps, as the sources that have faded will be difficult to recover from later surveys unless they brighten again in the future.

Additionally, J1642+6856 has also increased significantly, from  $2.75 \pm 0.13$  Jy to  $4.79 \pm 0.41$  Jy, with a large amount of scatter within our OCRA measurements over the last year implying ongoing variability.

### 5.2 WMAP sources

The subsample also has 42 sources in common with the 7-year WMAP point source catalogue (Gold et al. 2010). These are listed in Table 4, which gives the OCRA measurement and the WMAP K (23 GHz) and Ka-band (33 GHz) flux densities, and a comparison of the OCRA and WMAP Ka-band flux densities is plotted in Figure 3. Where there are multiple identifications for the WMAP sources (as given in Gold et al. 2010) the sources are marked with an “a”. Two CRATES sources – J1343+6602 and J1344+6606 – are separated by only 3.8 arcmin. Gold et al. (2010) list a single combined flux density for these sources. We also note that J1657+5705 had a Ka-band flux density of  $0.6 \pm 0.09$  Jy in Wright et al. (2009), but the flux density at this frequency is omitted in Gold et al. (2010).

The uncertainties of the WMAP flux densities were calculated from the scatter between the yearly WMAP measurements, and as such they combine the Gaussian and

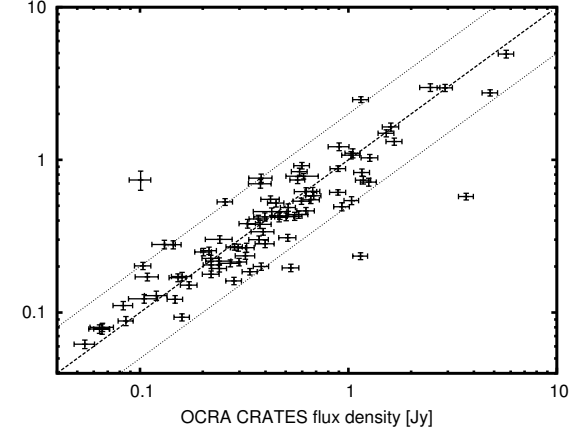


**Figure 2.** Comparison of common sources between CJF and CRATES. The dashed line is  $x = y$ ; the dotted lines indicate variability of a factor of two. The measurements broadly agree, with scatter ascribed to variability. Four sources particularly stand out as having varied significantly in flux density (see text).

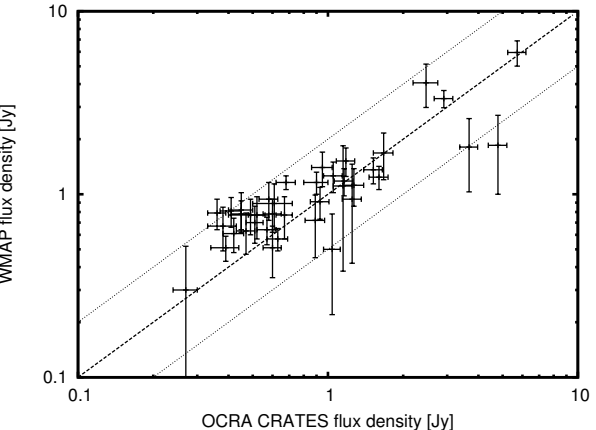


**Figure 3.** Comparison of OCRA-p and WMAP Ka-band measurements of common sources (as per Table 4). The paired sources, and the source with the missing flux density, have not been included. The dashed line is  $x = y$ ; the dotted lines indicate variability of a factor of two.

systematic errors as well as the source variability. The uncertainties on the OCRA-p measurements were calculated by the same method, although the measurements were taken over a shorter time period. There are 5 sources with a large uncertainty in both the WMAP and OCRA measurements – J1635+3808, J1642+3948, J1642+6867, J1849+6705, J1927+7358 – implying that these are variable on short ( $\sim$ year-long) timescales. Three sources have a large uncertainty in WMAP but not in the OCRA measurements – J1048+7143, J1638+5720 and J1727+4530 – implying that these are variable on longer timescales only, or were otherwise stable during the OCRA-p measurements.

At the lowest flux densities, we note that the WMAP flux densities are systematically higher than those from OCRA-p. These sources have likely been Eddington biased into the WMAP sample either by noise bias, variability or due to extra flux density seen by the large WMAP beam from nearby point sources, diffuse foreground emission or

Name	OCRA 30 GHz	WMAP K 23 GHz	WMAP Ka 33 GHz	Notes
	Flux density/Jy			
J1048+7143	1.15±0.10	1.21±0.61	1.11±0.73	
J1101+7225	0.93±0.08	0.92±0.16	0.91±0.18	a
J1302+5748	0.38±0.05	0.81±0.17	0.67±0.18	a
J1343+6602	0.32±0.03	0.70±0.17	0.34±0.13	Pa
J1344+6606	0.37±0.04	as above	as above	
J1419+5423	0.61±0.11	0.86±0.18	0.89±0.25	a
J1436+6336	1.04±0.08	0.68±0.23	0.50±0.28	a
J1549+5038	0.57±0.05	0.85±0.14	0.64±0.11	
J1604+5714	0.49±0.09	0.81±0.12	0.77±0.17	a
J1625+4134	0.45±0.04	0.96±0.06	0.78±0.14	
J1635+3808	2.47±0.28	3.72±0.86	4.06±1.08	
J1637+4717	1.27±0.12	1.10±0.26	1.12±0.26	
J1638+5720	1.67±0.15	1.67±0.43	1.68±0.48	
J1642+3948	5.72±0.48	6.60±0.90	5.95±0.94	
J1642+6856	4.79±0.41	1.82±0.68	1.85±0.85	
J1648+4104	0.45±0.05	0.67±0.08	0.82±0.20	a
J1653+3945	0.90±0.10	1.25±0.12	1.16±0.16	a
J1657+5705	0.51±0.04	0.41±0.10	—	
J1658+4737	0.68±0.06	1.16±0.10	1.16±0.10	
J1700+6830	0.39±0.05	0.32±0.07	0.51±0.08	
J1701+3954	0.52±0.04	0.58±0.09	0.77±0.20	
J1716+6836	0.60±0.05	0.58±0.11	0.51±0.16	
J1727+4530	1.25±0.11	0.89±0.44	0.94±0.52	
J1734+3857	1.05±0.09	1.20±0.11	1.26±0.24	
J1735+3616	0.51±0.04	0.71±0.09	0.70±0.16	
J1739+4737	0.67±0.05	0.86±0.12	0.77±0.20	
J1740+5211	1.16±0.10	1.22±0.26	1.18±0.20	
J1748+7005	0.47±0.04	0.50±0.15	0.63±0.16	
J1753+4409	0.42±0.04	0.63±0.21	0.61±0.13	a
J1800+3848	0.89±0.08	0.91±0.11	0.72±0.27	a
J1801+4404	1.18±0.10	1.36±0.26	1.52±0.27	
J1806+6949	1.52±0.13	1.42±0.14	1.36±0.22	
J1812+5603	0.27±0.03	0.21±0.11	0.30±0.22	
J1824+5651	1.60±0.14	1.47±0.26	1.24±0.18	
J1835+3241	0.41±0.04	0.81±0.09	0.81±0.15	
J1842+6809	0.95±0.09	1.29±0.27	1.40±0.30	a
J1849+6705	3.67±0.30	1.63±0.66	1.81±0.78	a
J1927+6117	0.58±0.05	0.95±0.26	0.94±0.22	
J1927+7358	2.91±0.25	3.57±0.27	3.33±0.36	
J2007+6607	0.63±0.06	0.78±0.09	0.57±0.08	
J2009+7229	0.60±0.05	0.64±0.12	0.78±0.16	
J2015+6554	0.36±0.03	0.75±0.14	0.79±0.15	a

**Table 1.** Comparison of 42 CRATES sources measured with OCRA-p that are also in the WMAP 7-year point source catalogue (Gold et al. 2010). The flux densities are given in Jy. Two sources – J1343+6602 and J1344+6606 – are combined in WMAP (denoted with “P”).

the CMB – a 50  $\mu\text{K}$  fluctuation in the CMB corresponds to  $\sim 0.25$  Jy at Ka-band in WMAP (Jarosik et al. 2010).

### 5.3 Fermi sources

We also carry out a cross-correlation of the CRATES sources with the Fermi-LAT 1 year point source catalogue (1FGL; Abdo et al. 2010a) and find 48 sources in common. The Fermi flux densities compared with the 30 GHz OCRA-p measurements are shown in Figure 4. We find a good correlation between the radio and gamma ray flux densities, most clearly indicated by the lack of sources with high radio flux densities and low Fermi flux densities. A Spearman-rank

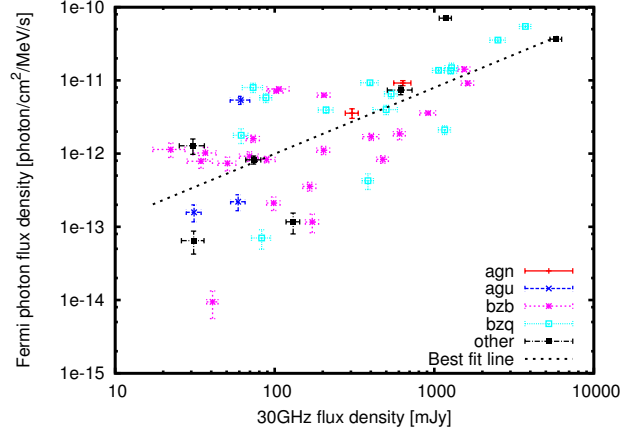


**Figure 4.** Comparison of the 30 GHz flux density from OCRA with the Fermi flux density for common sources. There is a surprisingly good correlation, shown by the line of best fit.

correlation test gives  $\rho = 0.71$  indicating a strong correlation (significant at greater than the 99.5% level); applying a best fit line of form  $\log_{10}(S_{30}) = m \log_{10}(S_F) + c$  gives  $m = 0.90 \pm 0.02$ ,  $c = -13.8 \pm 0.1$ . We split the sample up into different population classes using the classifications given in the 1FGL catalogue (i.e. BL Lac, quasar, etc.), and find no obvious dependency on population.

The above result is similar to that from the comparison between Fermi sources and the AT20G survey by Mahony et al. (2010) and Ghirlanda et al. (2010a,b), and also the comparison with the CRATES 8.4GHz measurements by Giroletti et al. (2010). We find a significantly higher correlation and slope than those comparisons, however we caution that sample bias will be present as CRATES is not a blind survey. It is also important to take the variability of both the gamma-ray and radio flux densities into account when interpreting this result, although this issue is lessened in this sample compared with AT20G due to the reduced separation in time between the gamma ray and radio measurements. In particular, Ghirlanda et al. (2010b) have shown that the slope of the relationship is strongly affected by selection effects and variability. Because we have not included sources with upper limits on their gamma-ray flux densities, the true slope of the correlation is uncertain but is likely to be steeper.

## 6 SPECTRAL INDEX DISTRIBUTIONS

The spectral index distributions for the CRATES sources between 1.4 and 4.8; 1.4 and 30; 4.8 and 30 and 8.4 and 30 GHz are shown in Figure 5. The effects of the selection criterion of  $\alpha_{1.4}^{4.8} > -0.5$  is obvious in the first of these. However, when flux densities measured at other frequencies are considered the effect of the selection cut becomes blurred. The mean and standard deviation for  $\alpha_{1.4}^{4.8}$  is  $0.00 \pm 0.38$ ; this changes to  $-0.27 \pm 0.29$  for  $\alpha_{1.4}^{30}$ ,  $-0.45 \pm 0.44$  for  $\alpha_{4.8}^{30}$  and  $-0.46 \pm 0.56$  for  $\alpha_{8.4}^{30}$ . This reflects the general steepening of the source spectra at high frequencies, as seen by e.g. Kellermann (1966); Ricci et al. (2006); Lowe et al. (2007); Massardi et al. (2008). We caution that the sample selection excludes sources with  $\alpha_{1.4}^{4.8} < -0.5$  and that, since the pri-

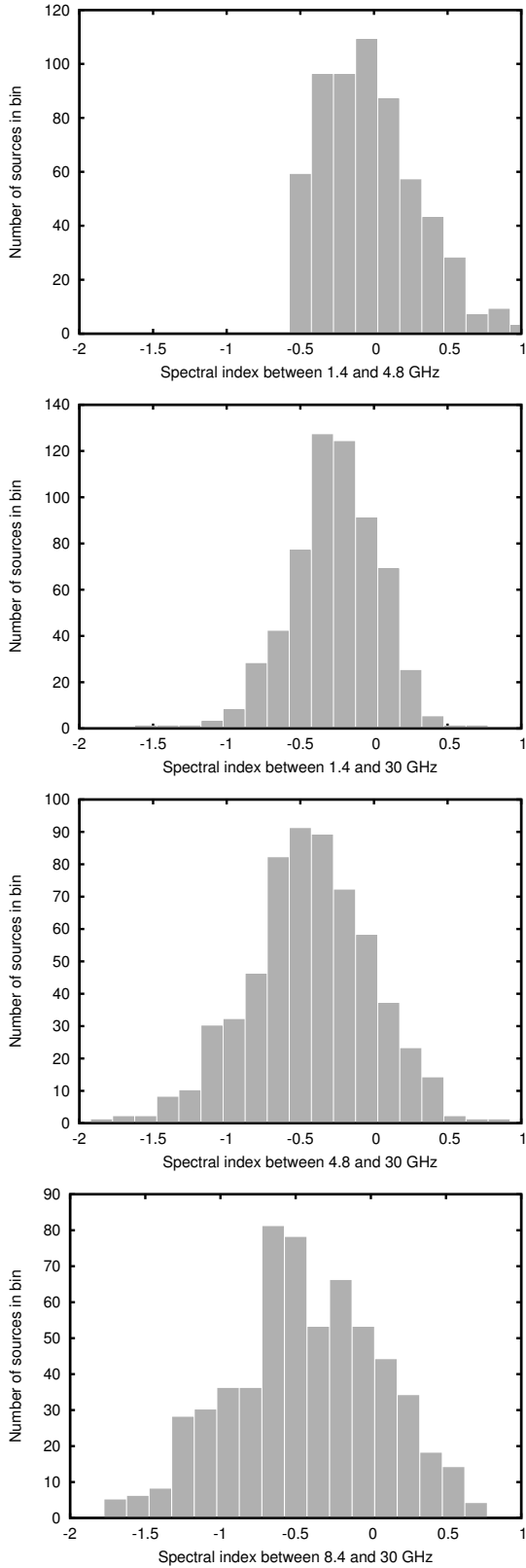


**Figure 5.** The spectral index distributions for the sources in the CRATES sample observed with OCRA-p. The hard cut-off in the first panel is due to the selection criteria of  $\alpha_{1.4}^{4.8} > -0.5$ .

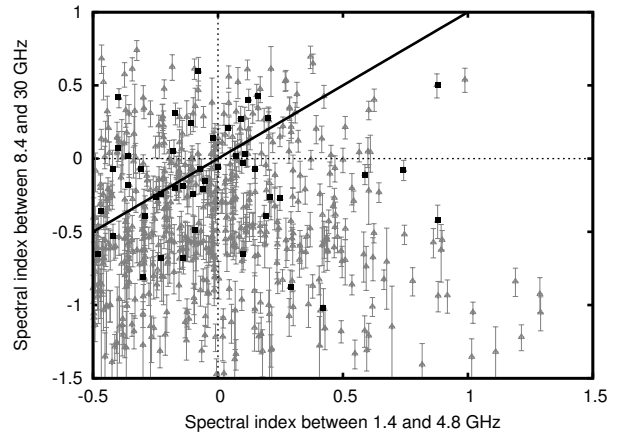


**Figure 6.** A 2-colour diagram for the CRATES source sample showing the spectral index from 1.4 to 4.8 GHz compared with the spectral index from 8.4 to 30 GHz. The solid line indicates  $x = y$ ; 75 per cent of sources have steepened and lie below this line. The darker points are sources also detected in the 1FGL (Abdo et al. 2010a).

mary selection frequency is 5 GHz, there is a bias against those sources that have spectra which flatten or turn up at frequencies above this.

The 2-colour diagram depicting  $\alpha_{1.4}^{4.8}$  vs.  $\alpha_{8.4}^{30}$  is shown in Figure 6. From this, we find that:

- 75 per cent of the sources have steepened at  $\alpha_{8.4}^{30}$  compared with  $\alpha_{1.4}^{4.8}$ ;
- 34 sources (6 per cent) appear to be Gigahertz-peaked sources that peak between 4.8 and 8.4 GHz (defined by  $\alpha_{1.4}^{4.8} > 0.5$  and  $\alpha_{8.4}^{30} < -0.5$ ; however see below);
- 63 sources (10 per cent) are flat or rising ( $\alpha_{1.4}^{4.8} > 0$  and  $\alpha_{8.4}^{30} > 0$ );
- 62 sources (10 per cent) are inverted ( $\alpha_{1.4}^{4.8} < 0$  and  $\alpha_{8.4}^{30} > 0$ ).

We caution that, due to the high resolution of the 8.4 GHz interferometric observations compared with the other measurements, sources that are extended or have multiple components will likely have underestimated flux densities at 8.4 GHz. This will have increased the number of sources with apparently rising spectra between 8.4 and 30 GHz. There are also some effects in the spectra due to the different resolutions and observational techniques at 1.4 and 4.8 GHz: e.g., although J1818+4916 and J1821+3602 have GPS-like spectra in the catalogue, the 1.4GHz flux densities do not include contributions from all the extended emission of these steep spectrum sources. Put another way, the GB6 observations overestimate the flux density of the compact components of these objects.

The sources cross-identified with the 1FGL catalogue (Abdo et al. 2010a) are shown as black squares in Figure 6. There is a tendency for these to have a flatter spectrum between 8.4 and 30 GHz than the rest of the sources, qualitatively in agreement with Mahony et al. (2010) and Ghirlanda et al. (2010a).

From a visual inspection of the spectra of the observed sources, combining the CRATES catalogue measurements with the OCRA-p measurements, and also available measurements in the literature (via the NASA/IPAC Extra-

Name	Cross ID	Notes
J0954+7435	VCS J0954+7435	d?
J1143+6619	–	
J1143+6633	VCS J1143+6633	cj?
J1144+6844	–	
J1210+6422	VIPS J12105+6422	d
J1245+7117	–	
J1247+7124	VCS J1247+7124	s?; C(M99)
J1305+5836	–	
J1333+6737	–	
J1336+7437	–	
J1338+6632	–	
J1436+4820	–	
J1443+6332	VIPS J14439+6332	d
	VCS J1443+6332	d?
J1446+6043	–	
J1457+6357	VIPS J14577+6357	cj?
J1525+6751	–	GPS(S98)
J1545+3941	VCS J1545+3941	GPS(M99)
J1549+6134	–	
J1558+6521	–	
J1613+4223	VIPS J16130+4223	s; C(M99)
J1613+6329	–	
J1614+5826	–	
J1619+7226	–	
J1624+6259	–	
J1628+4734	VIPS J16286+4734	cj; GPS(M99)
	VCS J1628+4734	
J1630+6659	–	
J1720+3604	–	
J1741+4751	VIPS J17415+4751	cj
	VCS J1741+4751	
J1756+5748	VIPS J17560+5748	t; GPS(M99)
	VCS J1756+5748 (t)	
J1757+4757	VIPS J17574+4757	s
J1800+3848	VCS J1800+3848	s; GPS(L07)
J1800+7325	–	
J1803+6433	–	
J1909+6241	–	
J1916+6053	–	
J1919+7240	–	
J1945+7055	VCS J1945+7055	c; GPS(S98)
J1955+6500	–	

**Table 2.** Candidate GPS sources, with VIPS (Helmboldt et al. 2007) and VLBA Calibrator Survey (VCS; Petrov et al. 2008) identifications and notes where the sources have previously been considered as Gigahertz-Peaked (“C” for Candidate, “GPS” for confirmed) by Snellen et al. (1998, S98), Marecki et al. (1999, M99) and Lowe et al. (2007, L07), and classifications of the morphology where interferometric maps are available (“s” for single, “d” for double, “t” for triple, “cj” for core-jet and “c” for complex).

galactic Database), we identify 38 candidate GPS sources, which are listed in Table 2. We also identify a further 29 potential GPS sources, which are marked in Table 3 with “G?”.

O’Dea (1998) and Lowe et al. (2007) found that  $\sim 10$  per cent of their 5 GHz-selected sources were GPS sources. We find fewer candidate GPS sources than this (6 per cent), but a similar percentage of combined candidate and potential GPS sources (11 per cent). We ascribe this to the difficulty in determining whether a source is GPS or not with fewer data points in the source spectra than is the case for the O’Dea (1998) and Lowe et al. (2007) samples. Addition-

ally, variable sources may appear to have GPS spectra as the measurements at each frequency have been taken at different epochs; as such, simultaneous measurements at different frequencies will be important to confirm whether these candidates are indeed GPS sources. Finally, there are some sources that have a rising spectra at all frequencies; these could be GPS sources that peak at frequencies greater than 30 GHz.

## 7 CONCLUSIONS

We have measured flux densities at 30 GHz for 605 flat-spectrum radio sources from the CRATES sample around the North Ecliptic Pole using OCRA-p and the 32-m Toruń telescope. These observations follow from those of the CJF sources by Lowe (2006) and Lowe et al. (2007), extending the work to lower flux densities. Where sources are in common, we find reasonable agreement between the measurements presented here and those by Lowe et al. (2007) and also WMAP (Gold et al. 2010). However, a number of sources display variability between the three sets of observations, and also within the present measurements. Such variability implies that simple source subtraction strategies in CMB studies can be subject to considerable uncertainty. We also find a good correlation (significant at greater than the 99.5% level) between the 30 GHz flux densities and the Fermi gamma-ray flux densities where sources are in common.

As expected, we find that the spectral index distribution for the sources broadens at higher frequencies. We ascribe this to the steepening of source spectral indices at different frequencies in different objects. We find 38 candidate Gigahertz-Peaked Spectrum sources, and also a significant number of inverted spectrum sources ( $\sim 10$  per cent). It is clear that extrapolation from low frequency flux densities to higher frequencies assuming power law spectra cannot be relied upon to produce accurate results. This emphasises the need for high-frequency blind surveys to low flux densities. Such surveys are currently being carried out by the ATCA at 20 GHz in the southern hemisphere (see e.g. Sadler et al. 2008) and AMI at 15 GHz in the northern hemisphere (Waldrum & Pooley 2004; Waldrum et al. 2010), and will be carried out by the OCRA-F instrument (Peel 2009) and its successors at 30 GHz in the near future.

The flux densities of the sources within the sample described here will be useful for comparison with point source measurements from the *Planck* satellite, which will make some of its most sensitive observations in the region covered here. The flat spectra of these sources should lead them to appear more frequently in the Planck bands than other classes of sources. This prediction will be tested, and a comparison of the measurements can be carried out, when the *Planck* Early Release Compact Source Catalogue is released in January 2011.<sup>1</sup>

<sup>1</sup> See <http://planck.ipac.caltech.edu/index.php?SiteSection=ERCSC>

## ACKNOWLEDGEMENTS

We are grateful for support of the OCRA project from a Royal Society International Project Grant. We are also grateful to the Polish Ministry of Science and Higher Education for their support of the OCRA project (grant number N N203 390434). This research has made use of the NASA/IPAC Extragalactic Database (NED) which is operated by the Jet Propulsion Laboratory, California Institute of Technology, under contract with the National Aeronautics and Space Administration.

## REFERENCES

- Abdo A. A., et al. for the Fermi-LAT Collaboration, 2010a, *ApJS*, 188, 405 (arXiv:1002.2280)
- Abdo A. A., et al. for the Fermi-LAT Collaboration, 2010b, *ApJ*, 715, 429 (arXiv:1002.0150)
- Battye R. A., Browne I. W. A., Peel M. W., Jackson N. J., & Dickinson C., 2010, preprint (arXiv:1003.5846)
- Becker R. H., White R. L., & Helfand D. J., 1995, *ApJ*, 450, 559
- Browne I. W. A., Mao S., Wilkinson P. N., Kus A. J., Marecki A., Birkinshaw M., 2000, in Butcher H. R., ed., Proc. SPIE Vol. 4015, Radio Telescopes SPIE, New York, p. 299
- Browne I. W. A. et al., 2003, *MNRAS*, 341, 13 (arXiv:astro-ph/0211069)
- Condon J. J., Cotton W. D., Greisen E. W., Yin Q. F., Perley R. A., Taylor G. B., Broderick J. J., 1998, *AJ*, 115, 1693
- Gawroński M. P. et al. 2010, *MNRAS*, 406, 1853, (arXiv:0909.1189)
- Ghirlanda G., Ghisellini G., Tavecchio F., Foschini L. 2010a, *MNRAS*(in press), preprint (arXiv:1003.5163)
- Ghirlanda G., Ghisellini G., Tavecchio F., Foschini L., Bonnoli G. 2010b, preprint (arXiv:1007.2751)
- Giroletti, M. and Reimer A., Fuhrmann L., Pavlidou V., Richards J. L. 2010, preprint (arXiv:1001.5123)
- Gold B., et al. 2010, preprint (arXiv:1001.4555)
- Gregory, P. C., Scott, W. K., Douglas, K., & Condon, J. J. 1996, *ApJS*, 103, 427
- Hafez Y. A., et al. 2008, *MNRAS*, 388, 1775
- Healey S. E., et al. 2007, *ApJS*, 171, 61 (arXiv:astro-ph/0702346)
- Healey S. E., Fuhrmann L., Taylor G. B., Romani R. W., & Readhead A. C. S. 2009, *AJ*, 138, 1032 (arXiv:0907.0788)
- Helmboldt, J. F., Taylor, G. B., Tremblay, S., et al. 2007, *ApJ*, 658, 203 (arXiv:astro-ph/0611459)
- Hill, R. S., Weiland, J. L., Odegard, N., et al. 2009, *ApJS*, 180, 246 (arXiv:0803.0570)
- Jackson, N., Browne, I. W. A., Battye, R. A., Gabuzda, D., & Taylor, A. C. 2010, *MNRAS*, 401, 1388 (arXiv:0912.0621)
- Jarosik, N. et al. 2010, preprint (arXiv:1001.4744)
- Kellermann, K. I. 1966, *ApJ*, 146, 621
- Lancaster K., et al. 2007, *MNRAS*, 378, 673 (arXiv:0705.3336)
- Lancaster K., et al. 2010, in prep.
- Lowe, S. 2006, PhD thesis, Jodrell Bank, University of Manchester
- Lowe, S. R., Gawroński, M. P., Wilkinson, P. N., et al. 2007, *Astronomy and Astrophysics*, 474, 1093 (arXiv:0707.3368)
- Mahony E. K., Sadler E. M., Murphy T., Ekers R. D., Edwards P. G., Massardi M. 2010, *ApJ*, 718, 587
- Marecki, A., Falcke, H., Niezgoda, J., Garrington, S. T., Patnaik, A. R. 1999, *A&AS*, 135, 273
- Massardi, M., Ekers, R. D., Murphy, T., et al. 2008, *MNRAS*, 384, 775 (arXiv:0709.3485)
- Myers, S. T., Jackson, N. J., Browne, I. W. A., et al. 2003, *MNRAS*, 341, 1 (arXiv:astro-ph/0211073)
- O'Dea, C. P. 1998, *PASP*, 110, 493
- Pazderska B. M., et al. 2009, *A&A*, 498, 463 (arXiv:0902.3945)
- Peel, M. 2009, PhD thesis, Jodrell Bank, University of Manchester (arXiv:1006.2760)
- Petrov, L., Kovalev, Y. Y., Fomalont, E. B., Gordon, D. 2008, *AJ*, 136, 580 (arXiv:0801.3895)
- Roukema B. F. 2010, *A&A*(submitted), preprint (arXiv:1007.5307)
- Ricci, R., Prandoni, I., Gruppioni, C., Sault, R. J., & de Zotti, G. 2006, *A&A*, 445, 465 (arXiv:astro-ph/0509580)
- Sadler, E. M., Ricci, R., Ekers, R. D., et al. 2008, *MNRAS*, 385, 1656 (arXiv:0709.3563)
- Snellen, I. A. G., Schilizzi, R. T., de Bruyn, A. G., et al. 1998, *A&AS*, 131, 435 (arXiv:astro-ph/9803140)
- Taylor G. B., Vermeulen R. C., Readhead A. C. S., Pearson T. J., Henstock D. R., Wilkinson P. N., 1996, *ApJS*, 107, 37
- Waldrum, E. M. & Pooley, G. G. 2004, preprint (arXiv:astro-ph/0407422)
- Waldrum, E. M., Pooley, G. G., Davies, M. L., Grainge, K. J. B., & Scott, P. F. 2009, *MNRAS*, 404, 1005 (arXiv:0908.0066)
- Wright, E. L., Chen, X., Odegard, N., et al. 2009, *ApJS*, 180, 283 (arXiv:0803.0577)
- Zijlstra, A., van Hoof, P. A. M., & Perley, R. A. 2008, *ApJ*, 681, 1296 (arXiv:0801.3327)

Table 3: Flux densities (in mJy) for the CRATES sources. See Section 4 for details.

Name	RA	Dec	$S_{1.4}$	$S_{4.8}$	$S_{8.4}$	$S_{30}$	Notes
	J2000		Flux density/mJy				
J0954+7435	09 54 47.5	74 35 57.1	1244.7	778	411.0	100.7±11.9	c,g
J1013+7427	10 13 30.7	74 27 26.9	125.8	87	63.4	106.2±11.7	
J1027+7428	10 27 24.1	74 28 26.1	190.1	211	143.5	72.0±9.8	
J1031+7441	10 31 22.0	74 41 58.3	213.2	250	103.9	123.0±12.3	
J1032+7218	10 32 31.9	72 18 18.9	121.4	100	71.0	62.6±7.1	
J1047+7238	10 47 47.5	72 38 13.0	36.7	108	31.2	58.3±6.1	f
J1048+7143	10 48 27.6	71 43 35.9	760.3	1900	1284.5	1148±100	w,f,c
J1056+7401	10 56 18.7	74 01 00.2	75.7	67	58.1	23.8±5.2	
J1056+7011	10 56 53.6	70 11 45.9	319.6	539	607.2	1031±102	c,v
J1059+7421	10 59 49.2	74 21 01.8	83.5	70	51.0	62.5±7.6	
J1101+7225	11 01 48.8	72 25 37.1	1281.2	858	366.7	930.0±80.4	w,c
J1107+7232	11 07 41.7	72 32 36.0	378.1	271	183.8	138.2±12.8	
J1113+6853	11 13 49.5	68 53 56.8	85.1	133	130.4	36.3±6.6	v, g?
J1127+7011	11 27 03.5	70 11 57.2	77.4	71	114.5	36.0±4.7	
J1128+6834	11 28 36.5	68 34 21.8	144.7	166	134.2	71.2±10.3	v
J1134+7249	11 34 11.4	72 49 20.0	222.3	229	214.4	32.7±3.3	
J1136+7009	11 36 26.4	70 09 27.3	328.1	267	213.7	163.4±15.5	f
J1141+6736	11 41 09.1	67 36 14.3	179.4	98	62.9	37.1±3.9	
J1143+6619	11 43 38.1	66 19 43.9	56.1	115	79.7	34.2±7.4	v,g
J1143+6633	11 43 41.6	66 33 31.2	133.5	245	275.7	60.7±5.8	g
J1144+6844	11 44 40.0	68 44 55.1	9.7	71	74.6	16.7±4.9	g
J1155+7316	11 55 27.5	73 16 35.6	48.2	86	65.4	39.7±4.5	
J1156+7306	11 56 27.3	73 06 50.2	312.4	172	144.9	66.2±7.0	2C
J1210+6422	12 10 31.6	64 22 17.5	56.2	146	97.3	5.4±2.8	g
J1211+7419	12 11 58.7	74 19 04.1	- <sup>2</sup>	115	14.0	13.9±2.3	e
J1215+6422	12 15 48.9	64 22 28.5	67.6	79	117.0	64.3±8.1	v,4C
J1219+6344	12 19 10.6	63 44 10.7	64.7	169	230.5	78.5±9.6	v
J1219+6600	12 19 35.8	66 00 31.9	77.1	111	329.9	162.7±16.1	7C
J1220+7105	12 20 03.6	71 05 31.1	258.8	293	188.1	81.7±11.2	f,v
J1220+7231	12 20 27.0	72 31 16.6	86.9	74	66.1	32.2±5.2	
J1220+6327	12 20 46.9	63 27 29.0	68.6	75	149.5	27.0±3.6	3C
J1220+6446	12 20 49.3	64 46 36.7	100.8	70	159.4	65.2±6.0	3C
J1226+6406	12 26 22.5	64 06 22.0	70	74	81.5	25.9±2.2	e,4C
J1229+6335	12 29 06.0	63 35 01.0	393.9	296	177.6	33.0±4.5	
J1231+6212	12 31 29.8	62 12 11.9	91.3	85	68.1	43.9±11.3	v
J1234+7232	12 34 33.0	72 32 37.3	106.2	88	143.8	77.4±8.4	
J1234+6745	12 34 53.8	67 45 49.3	129	99	55.5	62.6±5.5	
J1235+6853	12 35 19.3	68 53 37.6	129.3	76	44.7	20.2±3.5	2C
J1237+6128	12 37 35.5	61 28 09.9	86.3	68	60.7	29.4±9.1	e
J1240+6958	12 40 34.7	69 58 30.6	135.3	190	164.3	73.8±7.0	g?
J1243+7315	12 43 11.2	73 15 59.3	298.5	312	153.9	91.7±10.9	e,2C
J1243+7442	12 43 45.0	74 42 37.2	192.5	279	407.4	209.8±17.7	
J1245+7117	12 45 36.0	71 17 38.4	44.3	92	48.9	18.9±3.6	g
J1247+7046	12 47 07.6	70 46 45.1	95.2	91	115.6	86.3±9.3	
J1247+7124	12 47 09.3	71 24 20.0	120	194	104.5	7.7±1.2	g
J1247+6723	12 47 33.3	67 23 16.4	269.8	174	131.4	54.1±5.7	
J1248+5820	12 48 18.8	58 20 28.7	249.2	356	324.4	104.8±16.7	c,f,v
J1252+7326	12 52 37.9	73 26 21.8	143.2	88	45.7	13.3±3.2	
J1253+7357	12 53 09.0	73 57 29.3	174.8	111	34.6	52.0±7.1	
J1255+6124	12 55 45.0	61 24 50.9	99.4	97	47.8	30.3±4.6	3C
J1256+5652	12 56 14.2	56 52 25.2	309.5	415	256.5	119.9±14.9	c, g?
J1302+6902	13 02 37.9	69 02 51.6	234.4	194	159.4	225.4±18.4	
J1302+5748	13 02 52.5	57 48 37.6	327.4	601	861.5	381.4±48.6	w,c,v

Continued...

<sup>2</sup> The CRATES catalogue does not include a 1.4 GHz flux density for this source.

Name	RA	Dec	$S_{1.4}$	$S_{4.8}$	$S_{8.4}$	$S_{30}$	Notes
			Flux density/mJy				
J1304+6353	13 04 47.4	63 53 47.4	136.8	105	71.3	45.4±6.3	
J1305+5836	13 05 27.6	58 36 58.5	48.5	80	53.0	10.3±3.0	
J1306+5529	13 06 03.3	55 29 43.8	134.5	249	250.1	244.4±25.9	
J1308+5915	13 08 01.6	59 15 32.0	104.3	78	58.5	48.2±5.7	e
J1308+5530	13 08 54.5	55 30 47.6	85.3	94	65.8	72.5±7.9	e
J1309+5557	13 09 09.7	55 57 38.2	274.4	423	299.2	130.9±16.8	c
J1311+5513	13 11 03.2	55 13 54.3	433.3	487	498.2	144.4±13.1	c
J1316+6927	13 16 23.0	69 27 16.7	137.5	119	106.7	51.8±7.0	
J1316+6726	13 16 27.2	67 26 24.3	105.7	174	145.2	50.1±6.3	g?
J1316+7226	13 16 59.0	72 26 20.9	40.6	76	61.6	25.2±4.9	v, g?
J1317+6020	13 17 00.1	60 20 26.7	141.3	90	59.3	19.3±2.5	
J1317+6655	13 17 21.3	66 55 45.0	224.8	125	80.7	33.1±6.3	
J1319+6217	13 19 07.5	62 17 21.3	206.6	144	141.3	73.0±7.5	
J1323+6452	13 23 38.4	64 52 12.6	122.9	94	55.8	19.7±4.2	
J1328+6221	13 28 40.6	62 21 37.0	127.5	116	107.1	60.2±9.5	e
J1333+6737	13 33 46.2	67 37 20.1	36.8	79	39.0	16.3±3.0	g
J1334+5631	13 34 37.5	56 31 47.8	184.6	107	46.8	69.7±9.8	e
J1335+5844	13 35 25.9	58 44 00.3	295.1	740	747.9	381.8±32.1	c
J1336+7437	13 36 00.2	74 37 54.7	103.3	72	37.3	16.6±3.8	g
J1337+6532	13 37 16.1	65 32 46.3	215.5	128	248.5	176.5±18.5	
J1337+5501	13 37 49.6	55 01 02.1	724.9	753	559.1	376.3±49.7	c
J1337+5143	13 37 51.8	51 43 39.0	186	145	140.8	55.7±5.1	
J1338+6632	13 38 14.4	66 32 48.7	64.3	109	76.8	17.3±2.9	g
J1339+6328	13 39 23.8	63 28 58.4	492.3	419	277.2	66.1±8.5	c
J1340+6923	13 40 48.0	69 23 22.7	284	211	124.7	84.7±7.6	
J1341+7434	13 41 18.6	74 34 54.7	91.8	149	64.4	82.4±10.1	v
J1341+7054	13 41 45.4	70 54 48.9	51.2	74	34.5	24.4±2.0	e?
J1342+5110	13 42 24.3	51 10 12.4	151.6	129	137.4	68.9±9.9	
J1342+7212	13 42 51.7	72 12 53.7	81.6	78	65.3	28.4±2.9	
J1343+6855	13 43 00.6	68 55 17.2	213.5	204	173.6	53.0±4.7	
J1343+6602	13 43 46.0	66 02 25.7	221.7	299	595.8	320.9±26.4	w
J1343+5754	13 43 57.6	57 54 42.4	117.3	142	75.2	128.9±12.7	f
J1344+6606	13 44 08.7	66 06 11.6	660.1	545	499.2	372.8±40.1	w,c
J1344+5553	13 44 42.1	55 53 13.5	147.3	95	37.6	14.1±1.7	2C
J1349+5341	13 49 34.7	53 41 17.0	1108	644	764.3	577.2±61.2	c,v
J1350+6132	13 50 38.2	61 32 48.5	282.3	192	133.7	52.6±6.6	
J1350+6428	13 50 55.7	64 28 56.8	188.2	657	376.0	66.2±11.3	e, g?
J1351+5542	13 51 58.2	55 42 10.9	90.4	87	198.9	87.4±7.4	
J1353+6044	13 53 41.2	60 44 23.2	99.2	97	45.5	19.4±2.6	
J1353+6324	13 53 58.8	63 24 32.5	348.7	214	117.3	58.6±8.7	
J1354+6645	13 54 23.1	66 45 25.6	147.3	145	110.1	101.5±10.7	
J1354+7240	13 54 42.3	72 40 23.9	105.9	70	27.9	34.1±5.5	
J1359+5544	13 59 05.7	55 44 29.4	128.9	162	143.8	87.0±7.6	f
J1401+5835	14 01 45.7	58 35 42.3	145	209	204.3	69.6±6.3	
J1406+5822	14 06 55.5	58 22 00.0	112.7	109	86.6	89.1±9.3	e
J1408+5631	14 08 07.5	56 31 13.4	108.8	80	55.7	61.1±5.7	
J1408+5613	14 08 12.9	56 13 32.5	289.9	309	260.4	175.8±15.9	
J1408+6854	14 08 19.1	68 54 50.8	186.4	228	210.3	44.3±5.4	g?
J1410+6141	14 10 31.0	61 41 36.9	101.1	127	123.8	171.7±17.4	
J1410+6216	14 10 35.4	62 16 47.4	184.2	163	99.2	53.4±5.9	
J1411+5917	14 11 22.0	59 17 04.3	330.8	185	103.0	34.6±2.8	
J1411+7424	14 11 34.7	74 24 29.8	108.7	82	73.3	30.3±5.4	f
J1412+4844	14 12 38.7	48 44 47.1	66.4	74	41.2	52.8±5.0	
J1413+5305	14 13 24.3	53 05 26.9	142.9	141	66.4	70.7±8.1	
J1419+7315	14 19 41.2	73 15 04.3	92	66	26.2	6.0±4.9	
J1419+5423	14 19 46.6	54 23 14.8	802.5	1350	2248.1	609±108	w,c,f,v
J1421+4645	14 21 23.1	46 45 48.0	114.2	223	209.2	143.0±12.9	
J1421+5814	14 21 56.1	58 14 54.8	153.5	129	96.3	40.3±3.3	f,g?
J1422+4953	14 22 25.9	49 53 55.7	66.2	65	89.5	98.6±12.3	

Continued...

Name	RA	Dec	$S_{1.4}$	$S_{4.8}$	$S_{8.4}$	$S_{30}$	Notes
			Flux	density/mJy			
J1423+4802	14 23 06.2	48 02 10.8	408.5	515	399.3	201.7±18.6	c
J1423+7159	14 23 11.0	71 59 16.9	159	99	44.7	50.1±11.8	
J1423+5055	14 23 14.2	50 55 37.3	180	232	214.7	171.3±20.1	
J1423+5150	14 23 30.0	51 50 08.7	166.1	109	60.2	41.8±3.8	
J1424+4705	14 24 37.1	47 05 56.7	230.7	198	197.7	51.4±6.3	
J1426+5718	14 26 41.1	57 18 08.7	234.4	132	102	33.7±3.4	g?
J1428+5636	14 28 24.8	56 36 11.2	136.7	88	117.5	56.0±6.1	
J1428+4847	14 28 33.7	48 47 04.5	76.4	75	63.3	19.8±2.4	
J1429+6316	14 29 05.3	63 16 04.7	214.1	189	116.2	113.8±10.6	
J1429+5406	14 29 21.9	54 06 11.1	1043.1	716	494.2	219.4±20.3	c
J1429+6532	14 29 57.5	65 32 06.1	68.2	79	76.6	78.8±8.1	
J1431+7310	14 31 56.2	73 10 40.9	162.6	88	73.4	43.3±8.2	4C
J1433+6407	14 33 49.6	64 07 11.3	86	74	37.2	18.1±3.0	
J1434+5429	14 34 16.4	54 29 30.5	120.9	100	85.7	35.5±3.9	
J1435+5435	14 35 33.8	54 35 59.3	85.7	86	93.2	32.4±5.3	
J1436+4820	14 36 18.9	48 20 41.1	17.8	70	72.7	13.4±3.2	
J1436+6336	14 36 45.8	63 36 37.9	990.3	757	872.6	1035.7±83.0	w,c
J1437+5112	14 37 19.8	51 12 49.4	167.6	117	115.8	48.6±8.8	
J1438+4418	14 38 28.5	44 18 12.1	214.8	265	217.9	61.6±5.5	g?
J1439+4410	14 39 05.2	44 10 07.1	214.3	120	104.6	32.7±6.9	2C
J1439+4958	14 39 47.0	49 58 05.5	113.5	198	244.6	249.0±22.1	
J1441+6318	14 41 58.7	63 18 33.4	216.2	196	167.9	79.0±6.9	g?
J1442+5236	14 42 19.5	52 36 21.7	192.5	111	87.2	23.6±3.8	2C
J1443+5645	14 43 46.3	56 45 45.9	74.1	66	50.2	14.2±2.4	
J1443+6332	14 43 58.6	63 32 26.4	704.9	442	401.1	85.6±7.1	c,g
J1444+5538	14 44 22.8	55 38 16.5	128.7	75	79.2	101.9±11.6	
J1446+6043	14 46 51.8	60 43 13.0	131.6	81	53.7	12.3±3.4	g
J1448+5326	14 48 59.2	53 26 09.3	161.2	193	116.4	36.4±6.2	v, g?
J1451+6357	14 51 57.4	63 57 19.2	380	240	178.3	88.1±8.9	
J1452+4729	14 52 34.6	47 29 16.0	114.4	74	53.5	20.1±2.3	
J1452+5655	14 52 42.1	56 55 15.4	58.7	102	81.1	70.2±7.5	
J1452+5239	14 52 51.7	52 39 56.0	128.6	74	71	32.0±4.6	
J1453+5353	14 53 38.8	53 53 37.4	183.3	99	60.7	19.4±2.4	
J1454+4926	14 54 12.9	49 26 40.4	111.9	118	93.9	189.2±18.3	
J1454+5124	14 54 27.1	51 24 33.7	180	133	96.3	68.6±9.3	f
J1455+4431	14 55 54.1	44 31 37.7	198.1	192	164.2	98.5±12.2	
J1456+5048	14 56 08.1	50 48 36.3	226	232	259.2	64.0±5.3	
J1457+6731	14 57 16.5	67 31 18.9	93.4	120	93	25.7±3.5	g?
J1457+6357	14 57 45.6	63 57 07.7	38	104	88.4	14.5±2.9	g
J1459+4442	14 59 35.5	44 42 07.9	95	164	216.2	123.8±12.7	
J1459+4954	14 59 38.2	49 54 31.2	184	108	69	19.0±2.6	
J1500+4751	15 00 48.7	47 51 15.5	441.2	475	678	398.5±41.6	c,v
J1501+5619	15 01 24.6	56 19 49.7	174.3	99	51.7	37.4±3.8	3C
J1504+6856	15 04 12.8	68 56 12.8	135.8	227	76.9	35.8±5.8	e,4C
J1504+7147	15 04 53.5	71 47 25.3	110	86	85.9	34.6±6.7	
J1506+4359	15 06 05.9	43 59 03.0	86.7	93	101.3	87.6±8.4	
J1506+6226	15 06 38.2	62 26 49.8	123.3	70	32.4	12.8±3.2	
J1506+4933	15 06 44.1	49 33 55.8	98.3	137	217.4	420.7±35.9	
J1506+6620	15 06 48.0	66 20 58.9	137.4	107	76.5	44.4±4.7	
J1506+4239	15 06 53.0	42 39 23.0	384	405	412.6	659.9±65.7	c
J1507+5117	15 07 11.6	51 17 16.8	81.6	144	105.5	69.0±5.6	
J1507+5231	15 07 59.1	52 31 00.8	143.6	123	69.6	14.1±2.2	
J1509+5614	15 09 35.3	56 14 08.8	130.1	72	50.9	22.0±5.0	f,2C
J1510+5702	15 10 02.9	57 02 43.4	205.8	292	150.1	158.0±15.6	
J1512+4703	15 12 14.3	47 03 33.2	383.9	390	222.7	150.0±13.3	
J1515+5934	15 15 26.7	59 34 53.0	125.3	79	71.9	147.8±15.7	
J1518+5002	15 18 40.0	50 02 59.5	132.6	80	89.1	41.0±4.0	
J1519+4254	15 19 26.9	42 54 08.2	94.8	85	64.4	26.9±6.5	
J1520+5635	15 20 19.2	56 35 55.6	447.9	246	90	45.4±4.7	

Continued...

Name	RA	Dec	$S_{1.4}$	$S_{4.8}$	$S_{8.4}$	$S_{30}$	Notes
			Flux	density/mJy			
J1520+4211	15 20 39.7	42 11 11.5	139	85	56.5	60.8±6.4	f
J1520+4732	15 20 43.6	47 32 49.3	87.1	86	55.9	11.7±1.4	
J1521+4336	15 21 49.6	43 36 39.3	229.8	220	547.3	455.6±39.2	
J1524+7336	15 24 41.4	73 36 00.8	190	155	112.9	88.4±7.4	
J1525+4201	15 25 23.5	42 01 17.0	132.9	103	65.7	48.7±6.4	
J1525+6751	15 25 46.1	67 51 23.8	161.6	99	58.3	4.4±3.1	g
J1525+5828	15 25 48.3	58 28 51.3	110.1	71	34.3	50.0±4.1	
J1526+6650	15 26 42.9	66 50 54.6	90.5	404	305.7	64.0±7.2	c
J1526+6055	15 26 54.8	60 55 12.4	153.8	87	94.6	42.9±4.2	
J1527+5849	15 27 46.7	58 49 28.0	177	106	64.8	29.5±3.1	
J1527+4352	15 27 51.5	43 52 04.8	138.5	89	47.1	6.6±2.2	
J1528+6739	15 28 26.8	67 39 28.3	123.7	78	93.1	37.5±7.8	
J1528+4522	15 28 41.2	45 22 16.0	201.4	132	61.9	33.8±3.5	2C
J1529+7043	15 29 11.0	70 43 29.2	172.9	95	75.6	33.0±3.4	5C
J1529+6934	15 29 14.6	69 34 59.4	54.3	70	34.7	8.9±4.4	g?
J1530+5137	15 30 19.8	51 37 30.2	56.8	110	76.1	58.1±7.9	
J1531+5104	15 31 05.0	51 04 46.9	99.3	107	137.5	95.8±7.8	
J1531+5012	15 31 13.3	50 12 30.0	170.7	109	71.2	19.5±4.8	
J1531+7206	15 31 33.6	72 06 41.2	428.4	444	232.5	282.4±24.4	c
J1534+4823	15 34 04.9	48 23 40.9	319.4	204	73.1	45.0±4.0	2C
J1534+4920	15 34 32.6	49 20 49.2	85.7	84	112.7	43.9±4.8	
J1534+5839	15 34 57.2	58 39 23.5	129	119	136.8	25.5±2.3	
J1535+4836	15 35 14.6	48 36 59.7	106	163	101.4	76.6±9.2	
J1535+6953	15 35 19.2	69 53 18.4	88.5	67	123	17.0±6.2	
J1535+4957	15 35 52.0	49 57 39.1	214.6	367	306	152.2±14.3	c
J1536+3833	15 36 13.8	38 33 28.6	127.8	125	115.4	132.9±11.9	
J1536+3845	15 36 23.2	38 45 50.6	66.2	86	55.7	120.0±25.6	
J1539+5911	15 39 29.5	59 11 00.7	47.4	71	38.4	17.8±2.5	
J1540+6605	15 40 00.0	66 05 51.5	25.3	76	20.6	9.2±2.3	e
J1540+5803	15 40 37.6	58 03 34.4	65.9	71	70.5	52.5±7.2	
J1541+5348	15 41 25.5	53 48 13.0	240.7	248	113.8	165.8±15.8	
J1541+7401	15 41 28.9	74 01 47.7	154.6	102	55.1	53.0±7.1	2C
J1541+3740	15 41 35.9	37 40 51.1	95.8	83	48.2	39.1±7.8	
J1542+6129	15 42 56.9	61 29 55.4	89.1	121	144	100.9±10.4	f
J1543+6621	15 43 21.3	66 21 54.8	51.6	87	76	35.7±7.8	
J1545+5135	15 45 02.8	51 35 00.9	625.1	588	635.1	159.1±13.5	c
J1545+5259	15 45 04.9	52 59 25.5	211.9	122	64.2	39.8±5.6	3C
J1545+4751	15 45 08.5	47 51 54.7	691.6	437	343.6	65.8±5.8	c
J1545+5400	15 45 43.8	54 00 42.8	82.7	125	144.5	63.7±9.1	v
J1545+3941	15 45 53.2	39 41 46.8	196.9	310	76.8	1.8±1.7	g
J1546+5146	15 46 33.6	51 46 45.5	93.4	92	90.1	31.8±5.5	
J1548+6949	15 48 38.5	69 49 19.6	233.8	135	49.9	13.8±4.8	2C
J1549+5038	15 49 17.5	50 38 05.8	642.3	731	1286.1	570.6±46.6	w,c
J1549+6134	15 49 46.9	61 34 10.4	58.7	121	78.6	17.4±2.4	g
J1549+6310	15 49 57.3	63 10 07.3	70.6	91	43.1	30.6±4.9	f
J1550+4536	15 50 43.9	45 36 24.2	49.5	82	66.7	17.6±4.7	
J1551+5806	15 51 58.2	58 06 44.5	196	348	305.3	214.3±18.4	c
J1552+5552	15 52 10.9	55 52 43.2	106.2	94	131.3	192.0±28.1	
J1556+7420	15 56 03.0	74 20 58.2	184.7	138	120.6	158.9±14.5	
J1557+5440	15 57 21.4	54 40 16.0	97.2	85	48.4	43.6±7.0	e
J1557+4007	15 57 55.5	40 07 38.5	79	91	46.6	25.5±2.2	2C
J1558+6521	15 58 35.1	65 21 29.5	16.5	81	92.2	23.9±3.5	g
J1558+5625	15 58 48.3	56 25 14.1	210.2	206	169.7	199.6±18.7	f
J1559+5924	15 59 01.7	59 24 21.8	218.3	191	130.3	62.0±9.6	
J1600+7427	16 00 51.8	74 27 09.6	93.5	74	52.9	41.4±3.9	
J1602+4117	16 02 15.0	41 17 42.4	83.6	83	38.8	5.9±0.8	
J1603+6945	16 03 18.6	69 45 57.5	206.9	172	102.8	86.5±8.4	
J1603+6311	16 03 45.8	63 11 30.9	142.3	95	25.2	18.8±3.2	e
J1603+5730	16 03 55.9	57 30 54.4	340.5	365	308.9	153.3±19.3	

Continued...

Name	RA	Dec	$S_{1.4}$	$S_{4.8}$	$S_{8.4}$	$S_{30}$	Notes
			Flux	density/mJy			
J1604+5714	16 04 37.4	57 14 36.7	510.1	329	485.3	493.3±86.3	w,f
J1604+6722	16 04 46.2	67 22 17.0	68.2	68	45.5	34.7±5.1	
J1605+3722	16 05 33.8	37 22 51.1	140.7	125	97.6	46.8±5.3	
J1605+5931	16 05 50.2	59 31 43.4	138.1	114	170.7	148.1±17.6	
J1608+5613	16 08 20.8	56 13 56.4	248.9	236	180.8	139.5±14.6	
J1608+4012	16 08 22.2	40 12 17.8	207.5	240	127.9	274.0±23.5	e
J1609+5354	16 09 13.2	53 54 29.7	46.5	65	55.8	27.1±5.7	e
J1609+6532	16 09 14.0	65 32 29.0	67.5	88	73.2	13.8±6.0	6C
J1609+4717	16 09 35.6	47 17 56.3	88.9	88	76.1	52.9±6.2	
J1613+4223	16 13 04.8	42 23 18.9	42.1	200	133.5	5.0±1.5	g
J1613+6329	16 13 39.6	63 29 18.6	55.5	109	80	14.5±1.8	g
J1614+5826	16 14 58.3	58 26 08.9	13.3	65	67.3	20.5±3.1	g
J1615+4312	16 15 26.7	43 12 58.3	90.8	129	138.1	34.7±5.7	g?
J1616+4632	16 16 03.8	46 32 25.2	80.2	237	125.5	72.2±10.4	f,g?
J1616+6420	16 16 54.6	64 20 51.3	61.1	65	62.6	31.2±4.8	g?
J1616+3621	16 16 55.6	36 21 34.5	339.1	286	235.7	97.2±11.9	
J1617+4106	16 17 06.3	41 06 47.0	95.5	124	81.9	56.0±8.5	
J1617+5140	16 17 29.5	51 40 20.4	244.4	157	140.6	74.7±12.8	v
J1617+5150	16 17 44.4	51 50 54.2	101.2	93	93.7	10.9±2.2	
J1618+3717	16 18 26.6	37 17 11.5	106.1	68	53.1	24.8±3.7	
J1619+7226	16 19 37.7	72 26 32.5	172.3	119	58.9	11.5±3.2	
J1619+5256	16 19 42.4	52 56 13.4	185.1	128	181.8	54.2±5.8	
J1620+4901	16 20 31.2	49 01 53.3	448.1	442	401.3	298.5±26.2	c
J1620+5002	16 20 56.7	50 02 36.7	61.8	67	64	30.3±3.2	
J1622+3816	16 22 40.7	38 16 37.3	84.5	83	97.5	36.8±5.2	
J1623+6624	16 23 04.5	66 24 01.1	159.3	481	302.8	147.5±12.6	c
J1623+3909	16 23 07.6	39 09 32.4	184.9	244	219.4	26.8±5.7	
J1624+5741	16 24 24.8	57 41 16.3	534.3	585	594.4	502.8±43.9	c
J1624+5652	16 24 32.2	56 52 28.0	263.6	183	368.6	216.3±23.0	
J1624+6259	16 24 42.2	62 59 31.5	58.2	72	51.5	11.1±1.8	g
J1625+4053	16 25 10.3	40 53 34.3	165.2	110	86.6	86.5±11.1	2C
J1625+5715	16 25 32.9	57 15 42.5	45.4	67	60.2	104.1±11.3	
J1625+4118	16 25 42.2	41 18 41.1	80.8	107	76.8	65.8±7.1	
J1625+4347	16 25 53.3	43 47 13.8	127.4	123	71.8	51.5±7.9	
J1625+4134	16 25 57.7	41 34 40.6	1719.4	1253	1983.5	449.6±40.5	w,c,v,2C
J1626+5049	16 26 07.8	50 49 02.6	105.6	80	66.3	23.5±4.5	
J1626+5442	16 26 34.1	54 42 06.7	90.4	96	85.5	80.4±12.4	
J1626+5809	16 26 37.2	58 09 17.7	538.7	315	157.7	163.4±16.4	e,2C
J1627+4803	16 27 46.2	48 03 24.9	98.9	65	82.7	36.2±4.4	
J1628+4734	16 28 37.5	47 34 10.4	279.3	160	95.6	16.9±3.9	g
J1628+5641	16 28 49.5	56 41 14.5	156.3	119	134.1	190.9±21.8	
J1630+6659	16 30 34.9	66 59 05.5	148.3	98	59.3	13.1±1.9	g
J1630+5221	16 30 43.1	52 21 38.6	122.8	73	37.9	34.0±6.2	f
J1631+4927	16 31 16.5	49 27 39.5	319.2	422	657.1	428.3±78.6	c
J1631+5028	16 31 31.7	50 28 22.5	89.7	65	102.6	40.4±5.2	
J1631+4458	16 31 32.4	44 58 49.3	152	83	56.9	21.1±3.7	2C
J1633+6500	16 33 27.8	65 00 42.4	94.6	110	119.5	152.4±15.0	
J1635+3458	16 35 06.8	34 58 52.3	67	83	82.5	85.1±8.3	
J1635+3808	16 35 15.5	38 08 04.5	2799.7	3221	2403.9	2473±275	w,c,f,v
J1635+5955	16 35 37.7	59 55 15.1	163	232	108.5	167.1±15.9	
J1635+6019	16 35 37.7	60 19 56.7	457.7	248	156.1	40.1±4.4	g?
J1637+4717	16 37 45.1	47 17 33.8	1068.7	1244	766.7	1267±117	w,c,f
J1638+5720	16 38 13.5	57 20 24.0	1219.3	1750	1338.2	1660±147	w,c
J1639+5357	16 39 39.8	53 57 47.1	332.6	345	302	159.2±17.6	c
J1639+4705	16 39 56.0	47 05 23.6	234.4	136	108.7	69.7±7.7	e
J1640+3946	16 40 29.6	39 46 46.0	995.8	1117	1650.8	891.1±79.3	c
J1641+4006	16 41 31.2	40 06 51.0	94.9	69	58.2	29.6±6.0	v
J1641+3345	16 41 48.1	33 45 12.1	70.4	67	65.7	20.3±5.3	
J1641+5115	16 41 55.7	51 15 46.9	158.3	114	82	17.2±3.4	2C

Continued...

Name	RA	Dec	$S_{1.4}$	$S_{4.8}$	$S_{8.4}$	$S_{30}$	Notes
			Flux	density/mJy			
J1642+6856	16 42 07.9	68 56 39.7	1776.2	1527	1206.2	4786±409	w,c
J1642+6655	16 42 21.9	66 55 49.5	128.1	73	47.3	19.6±1.8	
J1642+3948	16 42 58.8	39 48 37.0	7270.8	8719	6299.8	5720±484	w,c,f,v
J1643+3448	16 43 40.3	34 48 05.4	137.8	86	58.3	13.6±3.2	
J1644+4546	16 44 20.0	45 46 44.4	184.7	109	64.6	47.4±5.0	2C
J1644+3916	16 44 34.5	39 16 04.9	120.8	77	73	27.9±4.5	
J1645+5233	16 45 26.4	52 33 35.6	168.2	92	44.4	39.4±6.6	e,v
J1645+4642	16 45 35.0	46 42 17.0	88.2	82	44.3	36.8±4.0	6C
J1645+6330	16 45 58.6	63 30 10.9	222.7	481	224.4	369.7±36.0	c
J1646+7419	16 46 15.2	74 19 11.1	386.3	249	177.9	60.2±8.4	v
J1646+4059	16 46 56.9	40 59 17.2	266	395	495.7	337.0±28.0	c
J1647+4950	16 47 34.9	49 50 00.6	181	191	232.3	301.3±28.2	f
J1648+6257	16 48 02.9	62 57 43.8	106.6	68	33.1	40.9±3.4	
J1648+4104	16 48 29.3	41 04 05.6	246.9	197	204.9	449.2±49.8	w
J1649+7442	16 49 41.0	74 42 44.6	99.2	108	128.9	127.0±21.1	
J1649+4857	16 49 58.0	48 57 15.4	82.4	68	62.3	20.4±2.5	
J1650+4140	16 50 05.5	41 40 32.4	237.5	136	85.1	41.3±5.1	
J1652+6232	16 52 01.5	62 32 09.1	46.1	85	48.7	19.7±2.7	
J1652+4013	16 52 33.2	40 13 58.3	90.1	111	104.2	57.2±5.0	e
J1652+3902	16 52 58.5	39 02 49.8	268	330	334.8	605.4±68.2	
J1653+3945	16 53 52.2	39 45 36.6	1625.8	1375	1158.4	903±104	w,c,f
J1655+4233	16 55 18.8	42 33 39.8	153.6	125	245.5	185.5±17.2	
J1655+5430	16 55 59.2	54 30 04.5	237.7	136	177.1	177.3±17.3	
J1656+5321	16 56 39.6	53 21 48.8	97	145	130.2	53.4±7.5	v
J1656+6012	16 56 48.2	60 12 16.5	299.6	184	226.5	379.0±31.3	f
J1657+5705	16 57 20.7	57 05 53.5	971.6	764	521.9	514.0±42.6	w,c
J1657+4808	16 57 46.9	48 08 33.0	1064	738	739.4	378.7±47.2	c
J1658+3443	16 58 01.4	34 43 28.4	464.2	474	378.5	258.4±26.5	
J1658+4737	16 58 02.8	47 37 49.3	868	1244	1186.4	681.0±57.0	w,c
J1658+6653	16 58 45.9	66 53 07.2	68	121	54.8	49.8±5.6	
J1659+5847	16 59 50.6	58 47 15.4	219.8	169	130.4	115.3±9.3	
J1700+6830	17 00 09.3	68 30 07.0	350.3	380	383.5	390.2±49.2	w,c,f
J1700+6612	17 00 59.2	66 12 27.5	131.5	91	82.9	78.3±6.3	
J1701+5133	17 01 22.4	51 33 49.7	117.4	93	92.9	62.7±7.6	
J1701+3954	17 01 24.6	39 54 37.1	195.6	150	285.4	516.8±42.0	w
J1702+5312	17 02 01.4	53 12 34.7	4.4	72	7.9	10.2±2.4	e
J1705+5109	17 05 26.4	51 09 35.4	336.1	184	143.7	64.4±6.7	e
J1707+4536	17 07 17.8	45 36 10.6	822.5	461	319.1	251.9±25.2	
J1708+3346	17 08 01.2	33 46 46.4	112.4	111	128.2	81.6±9.3	
J1709+4318	17 09 41.1	43 18 44.5	145.3	117	197.2	207.1±22.1	f
J1710+4848	17 10 04.3	48 48 31.1	48.3	86	52.5	28.6±2.5	
J1711+6853	17 11 20.2	68 53 01.7	61.4	115	105.3	136.6±13.4	
J1711+5411	17 11 40.5	54 11 45.1	222.3	172	208.6	153.6±13.3	
J1712+4655	17 12 01.3	46 55 57.7	110.4	118	85.9	20.5±3.4	
J1712+6053	17 12 12.4	60 53 28.9	25.9	91	130.7	33.9±3.1	
J1713+4916	17 13 35.2	49 16 32.6	208.1	183	231.2	229.8±25.2	2C
J1715+3619	17 15 08.4	36 19 50.2	92.9	93	55	62.4±10.2	
J1716+6836	17 16 13.9	68 36 38.7	507	838	819.7	595.6±53.8	w,c,v
J1716+4357	17 16 38.2	43 57 17.5	170.1	109	47.9	24.4±4.2	
J1717+4226	17 17 19.2	42 26 59.9	136	125	81.2	42.7±4.6	
J1717+3905	17 17 28.5	39 05 22.8	102.4	107	111.9	48.0±6.6	
J1718+4448	17 18 07.4	44 48 12.4	160.1	129	129.9	61.9±10.3	v
J1718+4228	17 18 15.2	42 28 18.3	112.3	86	62.7	52.4±5.1	3C
J1719+4858	17 19 14.5	48 58 49.4	147.8	164	206.7	199.4±16.8	
J1719+4804	17 19 38.3	48 04 12.3	64.2	109	188.1	15.7±1.4	
J1720+3604	17 20 03.6	36 04 17.4	33.3	70	72	14.7±2.0	g
J1721+3542	17 21 09.5	35 42 16.1	820.4	784	601.4	271.4±30.4	c,e
J1721+3233	17 21 43.3	32 33 16.9	81.4	89	86.9	39.8±5.4	
J1722+4339	17 22 35.4	43 39 21.2	76.1	79	89.1	43.6±5.2	

Continued...

Name	RA	Dec	$S_{1.4}$	$S_{4.8}$	$S_{8.4}$	$S_{30}$	Notes
			Flux	density/mJy			
J1722+5856	17 22 36.7	58 56 22.3	233.9	314	328	110.3±10.2	
J1722+6105	17 22 40.1	61 05 59.8	157.9	245	203.2	102.5±9.8	
J1722+6144	17 22 40.7	61 44 53.8	50	148	87	26.1±3.4	g?
J1722+5611	17 22 58.0	56 11 22.3	206.1	125	129.2	25.9±2.4	3C
J1723+6547	17 23 14.1	65 47 46.2	245.2	182	166	62.3±10.0	
J1723+3417	17 23 20.8	34 17 58.0	519	493	216	143.1±14.9	e
J1723+5236	17 23 39.8	52 36 48.4	523	334	245.6	129.6±14.9	2C
J1724+4004	17 24 05.4	40 04 36.5	576.8	524	296.1	627.2±77.1	c,f
J1724+3303	17 24 14.2	33 03 04.0	421.8	475	559.8	249.1±21.2	
J1724+4520	17 24 35.5	45 20 14.7	68.5	144	64	96.3±7.8	2C
J1724+6055	17 24 41.4	60 55 55.7	178.9	246	166	57.0±5.3	
J1724+4518	17 24 42.5	45 18 34.9	68.5	144	26.2	19.6±5.0	
J1724+4913	17 24 46.3	49 13 45.2	77.4	72	58.3	20.1±2.0	
J1725+4627	17 25 01.9	46 27 55.8	115.7	91	77.5	42.4±7.6	v
J1725+5301	17 25 30.5	53 01 27.2	52.5	110	46.4	48.7±6.3	e
J1726+6011	17 26 01.9	60 11 00.3	153.2	139	96.8	173.3±14.4	
J1726+3957	17 26 32.7	39 57 02.2	528.1	296	204.2	156.0±18.7	2C
J1726+3213	17 26 35.1	32 13 23.0	129.2	192	191.2	220.5±21.0	
J1726+4348	17 26 57.2	43 48 14.2	132.2	168	84.8	63.5±5.3	
J1727+5510	17 27 23.5	55 10 53.5	146.2	274	265.3	142.3±12.9	
J1727+4530	17 27 27.6	45 30 39.7	932.6	935	1360.3	1251±110	w,c,f,v
J1727+4703	17 27 35.5	47 03 30.2	39.7	68	62.8	27.6±4.1	e, g?
J1728+5013	17 28 18.6	50 13 10.5	207.6	145	161.8	97.2±9.4	f
J1728+3838	17 28 59.1	38 38 26.5	245.9	219	187	403.3±35.6	
J1730+3714	17 30 47.0	37 14 55.1	104.1	78	68.7	49.9±6.4	f
J1731+4617	17 31 57.1	46 17 18.8	273.1	149	84	19.5±2.6	
J1733+7046	17 33 12.5	70 46 29.8	79.4	71	8.3	12.9±2.2	e
J1734+3857	17 34 20.6	38 57 51.4	820.3	557	1160	1049.8±87.6	w,c,f
J1734+4625	17 34 30.3	46 25 53.1	41.9	95	111.1	38.4±3.3	g?
J1735+3616	17 35 48.1	36 16 45.6	341.6	334	958.7	506.3±40.7	w
J1735+5049	17 35 49.0	50 49 11.6	441.7	755	952	465.1±39.0	c
J1738+4008	17 38 19.1	40 08 18.2	78.1	113	152.3	135.6±19.4	
J1738+3224	17 38 40.5	32 24 09.1	164.1	142	294.1	72.1±6.3	
J1739+4955	17 39 27.4	49 55 03.4	538.6	428	577.7	552.7±46.0	c
J1739+3358	17 39 35.4	33 58 08.2	171.7	185	224.9	103.9±11.8	
J1739+4737	17 39 57.1	47 37 58.4	790.5	818	848.4	673.8±54.9	w,c,2C
J1740+4506	17 40 06.4	45 06 50.4	277.8	192	279.8	71.6±8.0	
J1740+5211	17 40 37.0	52 11 43.4	823.3	1699	1347.2	1162±101	w,c,f
J1740+4348	17 40 49.0	43 48 16.2	114.1	196	257	113.8±10.1	
J1741+4751	17 41 34.8	47 51 32.6	48.9	212	201.2	68.3±8.4	g
J1742+3742	17 42 02.2	37 42 13.2	120.9	70	48.1	5.0±3.8	g?
J1742+5741	17 42 04.7	57 41 58.5	63.4	70	26.4	50.7±6.8	
J1742+4633	17 42 16.7	46 33 26.2	140.9	98	64.7	25.6±3.7	
J1742+5945	17 42 32.0	59 45 06.7	108.5	88	116.2	169.8±16.1	f
J1743+3747	17 43 47.6	37 47 53.8	217.5	261	430	114.4±21.7	v
J1744+3259	17 44 14.5	32 59 29.4	93.6	77	56	46.6±7.2	
J1744+7356	17 44 31.4	73 56 14.0	129.1	70	55.8	13.8±6.1	
J1744+5542	17 44 56.6	55 42 17.2	580.8	562	305.6	241.3±35.5	c
J1745+5627	17 45 25.7	56 27 39.0	61.6	89	46.8	21.7±3.3	
J1745+4059	17 45 28.4	40 59 51.8	64	73	112.2	157.8±15.4	
J1746+6421	17 46 06.7	64 21 49.7	291.2	163	100.5	66.8±6.7	
J1746+6226	17 46 14.0	62 26 54.7	789.3	589	472.4	219.6±18.6	c
J1746+6048	17 46 26.8	60 48 22.8	138	101	92.4	54.0±5.7	
J1746+6920	17 46 30.0	69 20 35.6	154.5	140	138.4	142.4±13.2	
J1746+5341	17 46 32.5	53 41 31.5	86.6	116	56.4	32.1±5.1	
J1747+4658	17 47 26.7	46 58 50.9	312.4	669	882.3	240.4±19.7	c
J1747+7131	17 47 49.7	71 31 05.1	82	66	55.5	20.4±3.5	
J1748+3404	17 48 05.8	34 04 01.2	192.3	179	270.1	384.7±34.9	
J1748+7005	17 48 32.8	70 05 50.8	758	715	572.8	469.0±39.8	w,c,f

Continued...

Name	RA	Dec	$S_{1.4}$	$S_{4.8}$	$S_{8.4}$	$S_{30}$	Notes
			Flux	density/mJy			
J1749+4321	17 49 00.4	43 21 51.3	286.8	321	284.9	397.2±45.8	c,f
J1749+5241	17 49 39.0	52 41 16.0	115.9	77	43.5	12.6±1.9	
J1750+3231	17 50 31.2	32 31 50.5	47.2	79	63.2	38.2±7.8	
J1752+7311	17 52 11.7	73 11 20.5	124.5	163	141.9	161.3±13.8	
J1752+5819	17 52 17.2	58 19 57.6	63.6	73	37.2	19.3±2.7	
J1753+4409	17 53 22.7	44 09 45.7	787.7	1000	810.4	423.0±42.8	w,c
J1753+3427	17 53 29.9	34 27 08.2	99.4	65	38.1	18.5±1.5	2C
J1754+6452	17 54 07.6	64 52 02.6	145	257	192.4	87.8±7.5	
J1754+3540	17 54 13.7	35 40 48.5	243.1	204	135.6	60.8±9.8	
J1755+3350	17 55 11.2	33 50 59.8	147	139	134.6	46.1±5.5	
J1755+6905	17 55 21.4	69 05 29.1	78.3	78	54.1	28.5±3.0	
J1755+6236	17 55 48.4	62 36 44.1	294.7	203	147.5	78.4±6.6	
J1756+5748	17 56 03.6	57 48 48.0	770	463	282.8	54.4±6.1	c
J1757+5523	17 57 28.3	55 23 11.9	82.6	73	50.2	36.3±6.0	f
J1757+4757	17 57 28.4	47 57 24.4	117.9	153	112.5	21.1±2.9	g
J1759+5157	17 59 03.4	51 57 43.2	195.4	111	53.6	2.6±2.8	
J1759+4627	17 59 41.8	46 27 59.9	110.2	124	147.6	59.7±5.4	
J1800+3848	18 00 24.8	38 48 30.7	332.4	735	1211.2	892.5±76.3	w,c,g
J1800+7325	18 00 51.1	73 25 08.4	91	114	50.3	6.3±3.4	g
J1801+6051	18 01 11.6	60 51 13.7	134.6	107	98.8	48.2±5.0	
J1801+6902	18 01 14.6	69 02 43.8	228.2	130	79.8	48.2±5.7	
J1801+4720	18 01 21.4	47 20 58.0	97.1	84	58.5	50.0±4.9	
J1801+4404	18 01 32.3	44 04 21.9	746.9	1193	522	1179±99	w,c
J1801+5751	18 01 48.7	57 51 35.6	43.3	78	44.3	22.1±2.9	
J1802+4557	18 02 25.1	45 57 34.7	258.8	184	145.8	72.6±6.8	
J1802+7040	18 02 35.2	70 40 08.4	281.4	156	102.8	56.7±5.1	
J1803+6433	18 03 57.4	64 33 24.7	22.9	71	66.4	20.0±2.9	g
J1806+6141	18 06 19.9	61 41 18.3	268.9	328	196.1	299.8±30.7	
J1806+6949	18 06 50.7	69 49 28.1	1886.8	2122	1595.5	1520±132	w,c,f
J1807+5215	18 07 37.7	52 15 56.7	111.5	92	64.7	57.7±9.6	
J1808+3905	18 08 05.1	39 05 26.1	267.2	148	90.3	28.2±7.0	4C
J1808+3501	18 08 11.5	35 01 18.7	95.7	140	89.3	131.7±11.6	
J1808+4542	18 08 21.9	45 42 20.9	295.9	351	434.9	634.4±51.3	
J1809+4925	18 09 48.0	49 25 44.4	111.2	86	78.5	56.0±5.1	
J1809+3844	18 09 49.6	38 44 14.2	72.1	71	26	28.9±5.8	
J1810+5649	18 10 03.3	56 49 23.0	734	569	445.2	284.2±25.7	c
J1811+3751	18 11 42.3	37 51 49.6	143.2	87	103.9	123.4±17.4	
J1812+5603	18 12 57.7	56 03 49.2	161.7	255	112.7	269.7±26.2	w
J1813+3144	18 13 35.2	31 44 17.6	196.7	127	92	72.2±6.9	f
J1813+4721	18 13 50.6	47 21 14.7	137.2	78	14.1	27.1±3.9	e
J1814+4822	18 14 00.2	48 22 53.1	132.9	84	66.3	23.7±5.0	
J1814+4113	18 14 22.7	41 13 05.6	734.7	517	382.1	324.6±28.2	c,3C
J1814+6120	18 14 25.9	61 20 40.0	59.1	76	54.4	74.7±8.6	
J1815+4919	18 15 20.9	49 19 14.6	45.9	99	77.6	40.1±3.3	
J1815+4535	18 15 37.6	45 35 30.8	80.5	79	101.9	68.7±7.2	
J1816+4021	18 16 53.7	40 21 04.1	137.2	100	109.1	38.9±7.1	
J1816+5307	18 16 57.1	53 07 44.5	108.5	173	175	57.1±5.8	g?
J1817+5528	18 17 19.7	55 28 37.7	126.9	123	112.3	54.8±7.9	
J1818+4916	18 18 09.5	49 16 29.7	85.8	103	54.5	23.0±3.6	e
J1818+3520	18 18 12.5	35 20 26.4	207.9	136	99	23.1±2.3	
J1818+7157	18 18 22.8	71 57 44.5	131.4	76	56.2	39.0±5.8	v,2C
J1818+5017	18 18 30.5	50 17 19.7	180	130	239.2	124.0±11.3	
J1819+5511	18 19 10.1	55 11 08.6	77.8	67	64.6	45.9±6.5	
J1819+3845	18 19 26.6	38 45 01.8	63.9	91	128.6	196.0±19.2	
J1819+5424	18 19 49.3	54 24 28.8	55.6	66	39.4	22.0±2.2	
J1821+3602	18 21 03.4	36 02 25.4	98.5	205	94.5	17.6±2.9	e, g?,8C
J1821+6818	18 21 59.5	68 18 43.0	124.7	208	139.3	163.7±18.8	
J1821+3945	18 21 59.7	39 45 59.7	642.2	350	266.9	87.3±9.6	
J1822+5629	18 22 44.0	56 29 43.8	228	131	74.4	86.0±15.6	

Continued...

Name	RA	Dec	$S_{1.4}$	$S_{4.8}$	$S_{8.4}$	$S_{30}$	Notes
			Flux	density/mJy			
J1823+6857	18 23 32.9	68 57 52.6	223.9	187	207.9	222.3±25.5	
J1824+5651	18 24 07.1	56 51 01.5	1445.7	1263	1193.1	1598±144	w,c,f,v
J1825+5819	18 25 03.7	58 19 51.5	67.8	78	60.3	67.9±8.9	v
J1825+5753	18 25 41.6	57 53 05.9	150.3	201	167.7	66.9±8.8	
J1826+5437	18 26 08.2	54 37 19.5	142.2	102	61.8	90.6±10.2	
J1826+4402	18 26 17.3	44 02 55.7	128.1	75	80.2	56.2±6.0	2C
J1826+6706	18 26 37.5	67 06 44.7	126.1	71	26.4	62.3±7.7	
J1826+3431	18 26 60.0	34 31 14.1	482.1	331	289.4	173.9±17.4	
J1828+6434	18 28 09.9	64 34 16.0	231.6	270	222.6	153.6±12.4	
J1828+3220	18 28 56.9	32 20 04.1	70.1	90	16.7	19.9±4.9	e
J1829+6409	18 29 19.3	64 09 17.0	111.3	69	55.2	46.2±5.4	
J1829+3736	18 29 33.5	37 36 07.5	71.6	77	57.6	35.3±8.8	
J1829+3957	18 29 56.5	39 57 34.7	268.6	370	226.4	296.2±24.7	c
J1830+5816	18 30 53.9	58 16 16.2	77	80	47.1	6.4±1.5	g?
J1832+4041	18 32 40.8	40 41 12.3	121.2	113	145.7	108.3±10.1	
J1834+3205	18 34 49.1	32 05 25.4	89	80	117.3	50.9±7.2	
J1835+3241	18 35 03.4	32 41 46.8	112.6	2194	243.9	407.1±36.2	w,e
J1835+6203	18 35 12.5	62 03 41.7	200.9	195	7.1	11.4±2.7	e
J1835+6119	18 35 19.7	61 19 40.0	604.5	567	486.6	103.4±9.3	c
J1835+4904	18 35 21.8	49 04 43.6	118.9	65	50.2	20.3±3.6	2C
J1838+7331	18 38 19.9	73 31 54.9	144.8	111	66.6	33.5±3.4	
J1838+3253	18 38 37.7	32 53 51.0	101.5	101	140.7	106.8±13.9	
J1838+5210	18 38 50.7	52 10 54.0	100.4	73	32.9	23.7±4.2	
J1838+5735	18 38 58.6	57 35 39.3	89.4	93	66	54.2±7.6	
J1839+4100	18 39 05.8	41 00 59.1	208	160	124.1	73.5±6.6	
J1839+4236	18 39 49.2	42 36 06.0	109.6	94	61.6	87.3±13.2	v
J1840+6212	18 40 33.7	62 12 50.2	67	72	65.5	78.1±8.2	
J1840+3900	18 40 57.2	39 00 45.7	145.2	420	227.8	108.6±13.8	c
J1840+5452	18 40 57.4	54 52 15.9	209.7	252	201.1	183.5±23.5	
J1840+3702	18 40 58.6	37 02 29.2	63.2	100	85.1	83.4±6.8	
J1841+6718	18 41 03.9	67 18 50.0	179.3	167	99.2	47.8±7.1	g?
J1841+4129	18 41 10.1	41 29 41.1	49.1	83	54.9	26.4±3.6	
J1841+3711	18 41 15.1	37 11 51.4	327	217	80.6	120.5±31.5	v
J1841+6740	18 41 42.3	67 40 05.6	74.3	117	105.5	56.8±8.5	
J1841+3459	18 41 45.3	34 59 40.1	71.9	70	57.1	28.6±5.0	
J1842+5024	18 42 03.4	50 24 04.6	113.4	69	43.5	8.6±5.4	
J1842+6809	18 42 33.6	68 09 25.2	824.4	925	846.7	948.4±85.9	w
J1843+4449	18 43 07.9	44 49 51.5	118.4	90	103.3	143.4±19.6	
J1843+3225	18 43 29.3	32 25 27.5	274.1	160	160.9	75.6±10.7	
J1843+3558	18 43 51.4	35 58 35.4	125.6	151	63.8	47.0±11.4	2C
J1844+5709	18 44 51.0	57 09 38.6	164.7	123	83.1	59.5±4.9	
J1845+4007	18 45 11.1	40 07 51.6	1020.4	564	386.3	115.3±12.8	
J1845+5441	18 45 13.7	54 41 57.0	158.8	101	69	13.2±4.9	
J1845+3548	18 45 24.1	35 48 13.6	203	185	45	39.3±6.6	2C
J1845+3541	18 45 35.1	35 41 16.7	883.5	793	571.3	83.2±9.0	c,2C
J1845+5715	18 45 44.0	57 15 37.3	116.6	71	39.1	40.7±4.9	3C
J1846+7237	18 46 12.8	72 37 50.6	99.4	69	41	62.7±5.5	
J1846+3747	18 46 31.9	37 47 17.3	118.2	121	202.8	42.6±8.0	
J1849+6705	18 49 16.1	67 05 41.7	533.3	845	476	3675±301	w,c,f
J1849+7137	18 49 30.5	71 37 23.6	121.1	92	46.6	38.5±3.4	
J1849+5737	18 49 42.8	57 37 27.5	60.8	77	77.5	72.2±6.2	
J1850+4959	18 50 22.2	49 59 21.5	193.3	230	155.7	84.3±12.0	v
J1850+4057	18 50 31.3	40 57 31.4	119.4	99	84.8	37.6±5.5	
J1850+5744	18 50 37.9	57 44 12.7	82.7	102	34.8	18.2±1.6	
J1851+6100	18 51 52.4	61 00 38.8	269	219	189.6	176.5±14.6	
J1852+4855	18 52 28.6	48 55 47.5	242.7	311	374.1	529.5±48.8	c,f,v
J1852+4019	18 52 30.4	40 19 06.6	677.2	525	626.7	328.4±29.9	c,v,2C
J1852+4405	18 52 40.0	44 05 35.1	71	70	42	17.5±2.4	
J1854+7351	18 54 57.3	73 51 19.9	472.7	576	600.3	256.2±21.7	c

Continued...

Name	RA	Dec	$S_{1.4}$	$S_{4.8}$	$S_{8.4}$	$S_{30}$	Notes
	J2000		Flux density/mJy				
J1855+3742	18 55 27.7	37 42 57.0	189.7	367	227.6	75.2±6.5	
J1856+4400	18 56 59.3	44 00 14.6	142.9	84	94	26.0±3.5	
J1859+4431	18 59 18.8	44 31 29.4	66.3	72	59	10.2±5.5	e
J1901+6207	19 01 03.0	62 07 21.3	108.7	68	23.6	23.5±3.1	v
J1901+4858	19 01 08.7	48 58 13.9	28.3	65	25.5	10.3±3.5	e
J1902+4235	19 02 30.4	42 35 09.0	124.8	71	150	39.6±6.4	
J1903+5540	19 03 11.6	55 40 38.4	263.9	235	166.3	87.8±11.6	f
J1903+5130	19 03 13.1	51 30 31.1	95.2	84	113.3	102.9±11.0	
J1904+5355	19 04 33.8	53 55 08.4	84.4	75	72.5	21.3±2.9	
J1907+5141	19 07 37.5	51 41 57.3	114.4	105	62	29.4±3.2	
J1909+6241	19 09 20.2	62 41 38.8	146.5	113	80.5	17.2±2.8	g
J1909+4834	19 09 46.6	48 34 31.8	422.9	495	236.9	172.1±15.8	c
J1910+4802	19 10 34.2	48 02 11.8	244.3	154	126.1	142.1±15.4	
J1912+6526	19 12 06.0	65 26 30.1	83.4	71	45.6	42.6±5.5	
J1913+4706	19 13 16.0	47 06 49.7	164.8	108	17.3	37.3±3.8	e
J1915+6548	19 15 23.8	65 48 46.4	597.2	354	224.1	37.8±6.4	
J1916+6053	19 16 54.3	60 53 03.8	69	100	71.2	19.4±2.9	g,3C
J1918+5520	19 18 10.7	55 20 38.6	305.9	300	424.6	430.4±37.4	
J1918+4937	19 18 45.6	49 37 56.1	162.6	127	213.3	89.3±12.3	v
J1919+7240	19 19 53.9	72 40 58.6	53	66	51.1	9.5±1.9	g,4C
J1920+5350	19 20 01.3	53 50 46.8	115	96	91.9	50.6±6.8	
J1926+6921	19 26 37.9	69 21 14.9	115	85	108.6	35.9±3.9	8C
J1927+6117	19 27 30.4	61 17 32.9	546.2	558	514	582.9±50.6	w,c
J1927+7358	19 27 48.5	73 58 01.6	4040.8	3626	3697.8	2910±246	w,c,v
J1929+6146	19 29 35.1	61 46 29.3	215.4	121	117.1	72.8±7.9	f,5C
J1930+5859	19 30 20.9	58 59 11.4	23.1	78	69.6	136.5±14.3	
J1930+6627	19 30 46.2	66 27 37.4	31.4	74	40.5	9.3±3.9	
J1931+5227	19 31 33.1	52 27 19.3	110.9	95	115.2	52.0±5.6	
J1933+6540	19 33 57.3	65 40 16.9	225.1	240	285.6	235.9±20.5	
J1934+7117	19 34 15.4	71 17 51.8	182.9	116	116.3	66.1±5.4	
J1934+6138	19 34 40.7	61 38 41.6	198.5	140	235.3	192.0±16.2	4C
J1936+7131	19 36 03.6	71 31 31.8	570.6	398	497	320.7±34.2	c
J1937+7440	19 37 02.7	74 40 54.3	210.5	161	145.3	191.2±25.9	
J1937+6452	19 37 11.9	64 52 22.3	156.5	88	21.3	6.6±3.6	3C
J1937+6144	19 37 14.1	61 44 04.8	56.5	79	63.2	123.5±10.8	4C
J1937+5431	19 37 34.9	54 31 16.4	125.1	79	58.7	28.9±5.4	e
J1938+6307	19 38 16.2	63 07 17.8	243	182	124.8	138.8±15.6	
J1938+6648	19 38 25.3	66 48 52.9	587.3	329	214.2	66.8±5.7	4C
J1938+6300	19 38 37.4	63 00 29.8	220.4	124	95	111.3±9.7	6C
J1941+7221	19 41 27.0	72 21 42.2	237.7	165	171.9	60.4±8.5	f,3C
J1942+6307	19 42 57.2	63 07 37.8	248.7	157	175.5	121.3±11.5	8C
J1945+6015	19 45 10.6	60 15 02.7	16.6	88	65.8	6.9±2.4	
J1945+6534	19 45 45.7	65 34 45.7	117.1	91	71.4	18.6±3.0	
J1945+7055	19 45 53.5	70 55 48.7	974.3	677	482.6	240.0±33.2	c
J1946+6031	19 46 13.1	60 31 38.9	56	84	110.5	94.1±12.5	2C
J1947+6750	19 47 36.3	67 50 16.9	231.9	165	139.6	42.6±4.1	
J1949+7252	19 49 35.2	72 52 43.0	181.4	198	97.2	68.5±9.5	
J1950+7310	19 50 17.4	73 10 31.4	97.6	72	106.5	80.5±9.2	2C
J1951+5727	19 51 07.0	57 27 17.2	465.3	506	316.6	218.5±20.1	c
J1952+6501	19 52 10.0	65 01 46.2	89.8	113	73.4	34.5±6.5	
J1952+6234	19 52 35.5	62 34 04.4	200.5	123	80.9	93.3±7.8	2C
J1954+6153	19 54 56.0	61 53 58.3	62	127	186.7	9.6±2.7	g?
J1955+6500	19 55 17.4	65 00 44.2	71.6	78	40.5	10.7±3.1	g
J1959+6206	19 59 30.1	62 06 44.7	131.1	151	98.7	64.3±8.3	2C
J1959+6508	19 59 59.8	65 08 54.7	258.4	238	222.8	200.7±18.5	f
J2001+7040	20 01 34.0	70 40 25.8	161.1	96	61.1	30.8±3.3	f
J2004+7355	20 04 17.1	73 55 06.0	108	85	193.4	202.4±21.2	
J2006+6424	20 06 17.7	64 24 45.4	527.8	716	958	1142.9±93.2	c
J2007+7452	20 07 04.4	74 52 25.4	264.3	256	218.3	196.4±19.1	

Continued...

Name	RA	Dec	$S_{1.4}$	$S_{4.8}$	$S_{8.4}$	$S_{30}$	Notes
			Flux	density/mJy			
J2007+6607	20 07 28.8	66 07 22.6	522	749	480.9	626.0±60.3	w,c
J2008+6345	20 08 49.5	63 45 41.5	83.1	73	66.3	56.6±5.3	
J2009+7229	20 09 52.3	72 29 19.4	972.4	907	791.9	598.1±51.5	w,c,f,v
J2011+7205	20 11 03.8	72 05 12.2	139.8	137	113.1	53.2±7.5	g?
J2012+6319	20 12 22.0	63 19 12.0	125	125	111.3	131.3±11.0	
J2014+6553	20 14 32.0	65 53 55.4	542.5	337	224.8	88.9±7.9	
J2015+6554	20 15 55.4	65 54 52.7	680.2	529	553.6	363.8±32.8	w
J2016+6450	20 16 40.7	64 50 28.6	70.8	142	118.5	123.5±10.0	2C
J2017+7440	20 17 13.1	74 40 48.0	488.7	535	344.5	511.6±48.0	c
J2020+6524	20 20 02.3	65 24 45.4	81.7	65	92.5	47.6±6.8	3C
J2020+6747	20 20 18.9	67 47 06.4	243	163	257.5	114.8±12.1	2C
J2021+6418	20 21 36.0	64 18 47.4	149.8	145	131	65.5±5.9	
J2025+6616	20 25 15.8	66 16 12.8	58.7	73	82.7	1.6±2.0	g?,3C
J2045+7409	20 45 42.9	74 09 54.8	193	134	101.9	67.0±10.1	
J2051+7441	20 51 33.7	74 41 40.5	363.4	312	293.7	208.5±18.0	
J2052+6858	20 52 00.2	68 58 15.7	362.5	274	143.8	59.8±8.0	
J2103+7456	21 03 16.7	74 56 56.9	34.9	74	98.5	102.8±16.4	
J2107+7339	21 07 50.6	73 39 24.7	84.7	96	68.4	44.1±5.9	
J2125+7418	21 25 26.8	74 18 33.8	168.4	159	122.1	55.3±6.5	
J2132+7240	21 32 12.4	72 40 47.5	92.7	111	108.4	24.6±4.5	
J2205+7436	22 05 47.4	74 36 21.0	241.7	200	159.9	181.9±20.9	

This paper has been typeset from a T<sub>E</sub>X/ L<sup>A</sup>T<sub>E</sub>X file prepared by the author.z

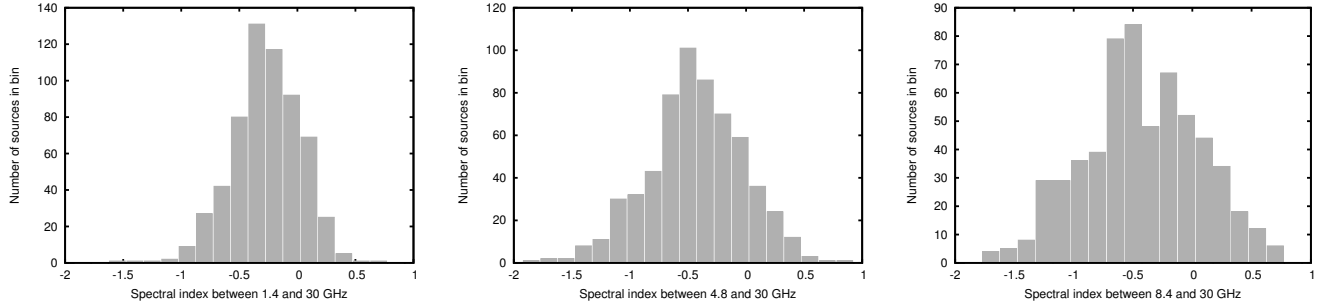


**Figure 7.** Updated spectral index distributions for the sources in the CRATES sample observed with OCRA-p; the difference from Figure 5 in the original paper is negligible.

## ERRATUM

In the paper ‘One Centimetre Receiver Array-prototype observations of the CRATES sources at 30 GHz’ (MNRAS, 410, 2690), an error was made in the application of the gain-elevation corrections for data taken between August 2009 and June 2010. As this error affected both calibrator and source measurements, it has resulted in an offset of up to  $1.75\sigma$  in the mean flux densities for some sources (or up to 25 per cent of the mean source flux density for the faintest sources). It also resulted in an increased scatter between the measurements, which led to a small overestimate of the uncertainty on the mean flux densities. The average change of all of the source flux densities is a decrease of 1.2 per cent. This is sufficiently small that our scientific conclusions are unaltered.

The updated spectral index distributions are shown in Figure 7, and the mean and spread for  $\alpha_{1.4}^{30}$ ,  $\alpha_{4.8}^{30}$ , and  $\alpha_{8.4}^{30}$  are unchanged from the values given in the paper. The other source statistics change slightly, as follows:

- (i) 76 per cent of the sources have steepened at  $\alpha_{8.4}^{30}$  compared with  $\alpha_{1.4}^{4.8}$ ;
- (ii) 33 sources (5.5 per cent) appear to be Gigahertz-peaked sources that peak between 4.8 and 8.4 GHz (defined by  $\alpha_{1.4}^{4.8} > 0.5$  and  $\alpha_{8.4}^{30} < -0.5$ );
- (iii) 63 sources (10 per cent) are flat or rising ( $\alpha_{1.4}^{4.8} > 0$  and  $\alpha_{8.4}^{30} > 0$ );
- (iv) 61 sources (10 per cent) are inverted ( $\alpha_{1.4}^{4.8} < 0$  and  $\alpha_{8.4}^{30} > 0$ ).

The application of the Spearman-rank correlation test of the Fermi-radio correlation using the revised mean flux densities gives  $\rho = 0.69$  compared to the previous value of  $\rho = 0.71$ .

An updated version of Table 1 (comparing the OCRA measurements to those by WMAP) is included below. We have provided an updated version of the flux densities in Table 3 in the Supporting Information, as well as online at <http://www.jodrellbank.manchester.ac.uk/research/ocra/crates/>.

Name	OCRA 30 GHz	WMAP K 23 GHz	WMAP Ka 33 GHz	Notes
	Flux density/Jy			
J1048+7143	1.14±0.09	1.21±0.61	1.11±0.73	
J1101+7225	0.93±0.08	0.92±0.16	0.91±0.18	a
J1302+5748	0.43±0.04	0.81±0.17	0.67±0.18	a
J1343+6602	0.32±0.03	0.70±0.17	0.34±0.13	Pa
J1344+6606	0.36±0.04	as above	as above	
J1419+5423	0.62±0.12	0.86±0.18	0.89±0.25	a
J1436+6336	1.04±0.08	0.68±0.23	0.50±0.28	a
J1549+5038	0.57±0.05	0.85±0.14	0.64±0.11	
J1604+5714	0.48±0.08	0.81±0.12	0.77±0.17	a
J1625+4134	0.45±0.04	0.96±0.06	0.78±0.14	
J1635+3808	2.47±0.28	3.72±0.86	4.06±1.08	
J1637+4717	1.27±0.12	1.10±0.26	1.12±0.26	
J1638+5720	1.66±0.15	1.67±0.43	1.68±0.48	
J1642+3948	5.72±0.48	6.60±0.90	5.95±0.94	
J1642+6856	4.78±0.41	1.82±0.68	1.85±0.85	
J1648+4104	0.46±0.04	0.67±0.08	0.82±0.20	a
J1653+3945	0.90±0.10	1.25±0.12	1.16±0.16	a
J1657+5705	0.51±0.04	0.41±0.10	—	
J1658+4737	0.68±0.06	1.16±0.10	1.16±0.10	
J1700+6830	0.39±0.05	0.32±0.07	0.51±0.08	
J1701+3954	0.52±0.04	0.58±0.09	0.77±0.20	
J1716+6836	0.60±0.05	0.58±0.11	0.51±0.16	
J1727+4530	1.25±0.11	0.89±0.44	0.94±0.52	
J1734+3857	1.05±0.09	1.20±0.11	1.26±0.24	
J1735+3616	0.51±0.04	0.71±0.09	0.70±0.16	
J1739+4737	0.67±0.05	0.86±0.12	0.77±0.20	
J1740+5211	1.16±0.10	1.22±0.26	1.18±0.20	
J1748+7005	0.47±0.04	0.50±0.15	0.63±0.16	
J1753+4409	0.42±0.04	0.63±0.21	0.61±0.13	a
J1800+3848	0.89±0.08	0.91±0.11	0.72±0.27	a
J1801+4404	1.18±0.10	1.36±0.26	1.52±0.27	
J1806+6949	1.52±0.13	1.42±0.14	1.36±0.22	
J1812+5603	0.27±0.03	0.21±0.11	0.30±0.22	
J1824+5651	1.60±0.14	1.47±0.26	1.24±0.18	
J1835+3241	0.37±0.03	0.81±0.09	0.81±0.15	
J1842+6809	0.95±0.09	1.29±0.27	1.40±0.30	a
J1849+6705	3.68±0.30	1.63±0.66	1.81±0.78	a
J1927+6117	0.58±0.05	0.95±0.26	0.94±0.22	
J1927+7358	2.91±0.25	3.57±0.27	3.33±0.36	
J2007+6607	0.63±0.06	0.78±0.09	0.57±0.08	
J2009+7229	0.60±0.05	0.64±0.12	0.78±0.16	
J2015+6554	0.36±0.03	0.75±0.14	0.79±0.15	a

**Table 4.** Comparison of 42 CRATES sources measured with OCRA-p that are also in the WMAP 7-year point source catalogue. The flux densities are given in Jy. Two sources – J1343+6602 and J1344+6606 – are combined in WMAP (denoted with “P”).